MICROFACIES OF STROMATOLITIC SINTER FROM ACID-SULPHATE-CHLORIDE SPRINGS AT PARARIKI STREAM, ROTOKAWA GEOTHERMAL FIELD, NEW ZEALAND

Richard Schinteie, Kathleen A. Campbell, and Patrick R.L. Browne

ABSTRACT

We present a unique, scale-integrated, and spatially controlled study of acid-derived sinters and their abiotic-biotic relations. Through a microfacies-based approach, we provide context and constraints for inferring causal factors in the formation of these sinters. Four distinct microfacies of siliceous stromatolitic sinter formation and their associated microbiota were elucidated from acid-sulphate-chloride hot spring outflows (pH 2.1-2.3, 91-30°C), located on the floodplain of Parariki Stream, ~1 km north of Lake Rotokawa in the Rotokawa Geothermal Field. *Microfacies 1* comprises cup- to ridge-shaped sinters forming close to vents (91-64°C) with relatively high water and gas discharge. Sinter surfaces are characterised by relatively small (0.5 cm high) spicules, irregular, gnarly siliceous textures and colonisation by coccoidal microorganisms (1-1.5 µm in diameter). *Microfacies 2* consists of spiculose (1 cm high) sinters colonised by bacilli (1-2.3 µm long), diatoms and coccoidal algae (2–10 µm in diameter) that are surrounded by quiescent waters (85-30°C) with little steam discharge. *Microfacies 3* is typified by parallel-laminated sinters forming on slightly steepened areas that are colonised by bacilli (1-8 µm long), diatoms and coccoidal algae (2–10 µm in diameter) and exposed to fluctuating water levels (60-54°C). *Microfacies 4* constitutes thin siliceous sinter rims forming mainly on small pumiceous clasts that rest upon moist (67-45°C) sandy substrates and colonised by bacilli (1-2.3 µm long), diatoms and spherical cells (2-6 µm in diameter). Sinter morphology, texture and formation mechanisms, as well as microbial colonisation, depend on a variety of environmental constraints that can act at a scale of centimetres or less. Textural development of the sinters, including their laminae, is attributed to a combination of abiotic and biotic factors. The differential preservation potentials of microbial communities need to be taken into account when assessing biodiversity of ancient sinters.

Richard Schinteie. Geology Programme, School of Geography, Geology and Environmental Science, University of Auckland, Private Bag 92019, Auckland 1142, New Zealand. Currently: Research School of Earth Sciences, Building 61, Mills Road, The Australian National University, Canberra A.C.T 0200, Australia.
richard.schinteie@anu.edu.au

Kathleen A. Campbell. Geology Programme, School of Geography, Geology and Environmental Science, University of Auckland, Private Bag 92019, Auckland 1142, New Zealand.
ka.campbell@auckland.ac.nz (corresponding author)
Patrick R.L. Browne. Geology Programme, School of Geography, Geology and Environmental Science, University of Auckland, Private Bag 92019, Auckland 1142, New Zealand.
prl.browne@auckland.ac.nz

INTRODUCTION

Stromatolites may serve as important proxies for early life on Earth. Many modern siliceous hot spring deposits, or sinters, have laminated growth structures that characterise such stromatolites (e.g., Walter et al. 1972; Doemel and Brock 1974; Renaut et al. 1998; Jones et al. 2000, 2005; Konhauser et al. 2001; Campbell et al. 2002; Guidry and Chafetz 2003; Handley et al. 2005). Sinters are often colonised by a range of (hyper)thermophilic microbiota that can become silicified and incorporated into these deposits (e.g., Inagaki et al. 2001; Blank et al. 2002; Walker et al. 2005). The taxonomic identities of these microbes can vary within and between different geothermal settings, and are a result of the numerous niches and (micro)habitats encountered in these localities (e.g., Schinteie 2005; Pancost et al. 2005, 2006). Microbes inhabiting thermal environments are often placed at the most deeply rooted parts of the universal tree of life (e.g., Barns et al. 1996; Stetter 1996; Pace 1997; Hugenholtz et al. 1998). Hence, the mineralisation of sinters and the phylogeny and ecology of hot spring microorganisms are central themes in studies concerning the origin of life, astrobiology and mineral-microbe interactions (e.g., Walter and Des Marais 1993; Henley 1996; Farmer and Des Marais 1999; Farmer 2000; Handley et al. 2005). Indeed, hot spring deposits, like sinters, may have provided surfaces that concentrated organic chemical constituents, thereby contributing to the formation of biological membranes important for the origin of life (Henley 1996).

Studies concerned with the formation of sinter and the distribution of their associated microbiota require an understanding of the different litho- and biofacies occurring at hot spring sites (Farmer 2000). The deposition of actively forming sinters and the occurrence of specific microorganisms are affected by shifting environmental parameters that result in zonations around hot spring effluents with respect to sinter morphology, texture, and microbial species composition. In particular, deposits of sin-

ter and their microbiota can act as sensitive indicators of pH-temperature conditions (e.g., Brock 1978; Cassie and Cooper 1989; Cady and Farmer 1996; Lowe et al. 2001; Jones et al. 2000; Jones and Renaut 2003; Lynne and Campbell 2003, Rodgers et al. 2004) and the hydrodynamics of spring discharge (e.g., Jones and Renaut 1997; Braunstein and Lowe 2001; Lowe et al. 2001; Guidry and Chafetz 2003; Lowe and Braunstein 2003). From observed variations in the texture and distribution of sinters, and the species composition or cell morphology of the associated microbiota, facies models have been constructed to characterise surficial deposits from alkali-chloride hot springs (e.g., Walter 1976; Cady and Farmer 1996; Farmer 2000; Campbell et al. 2001; Guidry and Chafetz 2003; Lowe and Braunstein 2003).

While ancient sinters from extinct hot springs may retain some primary textural characteristics (e.g., Rice et al. 1995; Walter et al. 1996; Trewin et al. 2003; Campbell et al. 2001, 2004), their palaeoenvironmental signatures commonly are obscured by the loss of fine-scale microstructure due to diagenetic overprinting (Cady and Farmer 1996) or differential preservation (Guidry and Chafetz 2003). In addition, interpreting ancient sinter facies requires an understanding of the relative contributions of abiotic and biotic factors in the formation of a variety of sinter textures. However, studies of modern, actively forming sinters allow for such shortcomings in palaeoenvironmental reconstruction to be addressed (Farmer 1999).

While most investigations are of sinters deposited from thermal waters of near neutral pH, very few (e.g., Jones et al. 1999, 2000; Mountain et al. 2003; Rodgers et al. 2004) have addressed sinters formed from highly acidic (pH ~3 or lower) hot spring waters. Such studies could potentially enable the recognition of extinct hot spring systems and their deposits, even where there is no longer any evidence of the original discharging waters. Indeed, acid hot spring deposits may be the most appropriate terrestrial analogues for the

recognition of extraterrestrial hydrothermal deposits. Acidic hydrothermal fluids and solphatara-like environments may occur on Mars (e.g., Farmer 1996, 2000; McCollom and Hynek 2005). In addition, numerous landforms and sedimentary features observed on Mars appear to have equivalents in acid environments on Earth (Benison and Laclair 2002; Laclair and Benison 2002; Bullock 2005). Chemical and mineralogical data obtained from previous Mars missions also paint a picture of acid alteration (e.g., Benison and Laclair 2002; Kerr 2004; Bullock 2005; McCollom and Hynek 2005).

This study aims to further contribute to the understanding of acid-derived sinters. We investigated microfacies (i.e., facies changes over centimetres or less) of siliceous stromatolitic sinters formed in acid-sulphate-chloride spring outflows (91-30°C, pH 2.1-2.3) located on the floodplain of Parariki Stream, Rotokawa Geothermal Field, New Zealand. This field provides a rare setting where acid fluids rich in silica deposit sinter. The deposits follow strong environmental gradients that result in distinctive morphological, textural, and microbial characteristics. Molecular, DNA-based surveys at the site have shown that microbial communities vary markedly with respect to species composition between different microfacies (Schinteie 2005). Sequences of 16S ribosomal RNA (rRNA) genes were extracted from individual sinters and were related to numerous archaeal, bacterial, and eukaryotic thermoacidophiles. The results of this molecular survey are the subject of a different contribution that closely ties in with the results outlined herein.

We employed an integrative approach with the application of: (1) detailed mapping of sinter occurrences with respect to temperature, hydrodynamics of spring discharge, and sinter formation rates; (2) X-ray powder diffractometry (XRPD) to characterise sinter mineralogy; (3) thermal analysis for investigating water content of the sinters; (4) thin-section petrography for recognising broad sinter textures; and (5) Scanning Electron Microscopy (SEM) to resolve textural micro-structures and mineral-microbe relationships. Treatment of fresh sinter samples with glutaraldehyde slowed the deterioration of associated microbial communities, lessened the risk of contamination by post-collection microbial overgrowth, and better illuminated the role of microorganisms in acid-derived sinter texture formation (cf. Cady and Farmer 1996; Lynne and Campbell 2003; Handley et al. 2005).

MATERIALS AND METHODS

In 2004, the study site was mapped to determine sinter microfacies types, vent locations, fluid flow directions, temperatures, and pHs of discharged thermal waters, water level changes, and silica accretion rates. The site was visited several times that year to note any environmental changes, especially of water levels. Mapping was undertaken with tape and compass. Temperatures and pHs were measured with a portable battery operated Orion^{TM} (model 250A) pH/ISE meter with automatic temperature compensation. Silica accretion rates were measured by placing glass slides (25 x 75 mm) vertically in the discharge channels for 67 days (cf. Mountain et al. 2003; Handley 2004; Handley et al. 2005). Filtered (<0.2 μm) water samples were collected in February 2006 to determine anion (unacidified) and cation (acidified by 0.5% HNO_3) concentrations. For HCO_3 and H_2S concentrations, samples were collected in rubber-sealed bottles. The waters were analysed by the Institute of Geologic and Nuclear Sciences (IGNS), New Zealand.

The silica mineralogy of the sinters was determined by X-ray powder diffractometry (XRPD). Each sample was air-dried and ground to a fine powder in a mortar and pestle. XRPD was conducted with a Philips diffraction goniometer fitted with a graphite monochromator. Samples were scanned at 1.95° 2θ/min with a step size of 0.02° from 2 to 62° 2θ. Operating conditions were 40 kV and 20 mA using CuKα radiation (λα1 = 1.54051 Å; 2 = λα1.5443 Å).

Sinter composition and water content was determined by combined differential thermal analysis (DTA) and thermogravimetric analysis (TGA). Sinters were air-dried, ground to a fine powder, placed into pre-weighed platinum crucibles (~0.22 g), and heated to 1400°C in a Polymer Laboratories Simultaneous Thermal Analyser 1500 (Epsom, Surrey, UK) equipped with PLus V software (v.5.40) and a type R (Pt-13% Rh/Pt) flat-plate thermocouple system. Heating was in dry air or nitrogen. The former allowed the combustion of organic material to be gauged, while the latter measured water loss.

Fine-scale sinter textures and potential microbial involvements were examined by Scanning Electron Microscopy (SEM). Samples were stored in a fixative of 2.5% glutaraldehyde immediately upon field collection. Prior to imaging, samples were critical-point dried to prevent the effects of surface tension from destroying delicate biofilms.
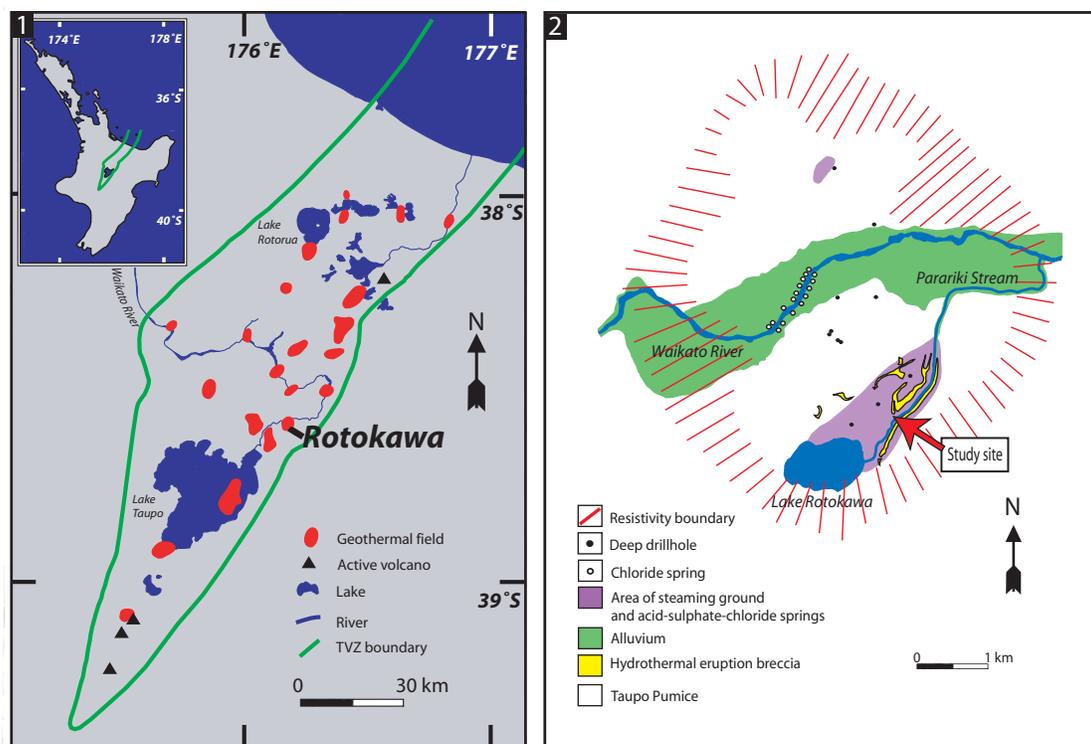
Figure 1. Study site location. (1) The Taupo Volcanic Zone and associated geothermal fields in the central North Island, New Zealand. Modified from Bibby et al. (1995) and Wilson et al. (1995). (2) Map of the Rotokawa Geothermal Field and location of the study site. Modified from Collar and Browne (1985), Krupp and Seward (1987) and Reyes et al. (2002).

The samples were rinsed twice in deionised water followed by dehydration through an ethanol series (30%, 50%, 70%, 90%, and 100% x 2). Ethanol was exchanged for liquid CO_2 at 5500 kPa by flushing and soaking for one hour in a Polaron E3000 Series II critical point drier (Polaron Equipment Ltd, Watford, UK). Liquid CO_2 was subsequently vaporised at 31.5° C. Critical-point dried samples were mounted on aluminium stubs and coated with platinum using a Polaron SC 7640 Sputter Coater (Quorum Technologies Ltd, Newhaven, UK). Samples were examined with a Philips SEM XL30S (Eindhoven, Netherlands) fitted with SiLi (lithium drifted) electron-dispersive X-ray spectrometer (EDS) with a Supra Ultra Thin Window (EDAX, Mahwah, New Jersey, USA) for assessing elemental composition of sinter components.

To examine broad sinter textures and allow for comparisons with fine-scale SEM images, thin sections of the sinters were constructed. Samples were first embedded overnight in an epoxy resin of methyl methacrylate, and the dried resin was subsequently polymerised using cobalt-60 radiation. Sections were examined under a Nikon Labophot-

POL petrographic microscope (Tokyo, Japan) equipped with a Nikon Coolpix 4500 digital camera (Tokyo, Japan).

SETTING AND SITE DESCRIPTION

The Rotokawa geothermal field is situated in the southeastern margin of the Taupo Volcanic Zone, North Island, New Zealand (Figure 1.1). The field covers an area of ~6 km^2 that is characterised by steaming ground, fumaroles, hot springs, mud pots, collapse pits, and infilled hydrothermal eruption craters (Figure 1.2) (Browne 1974; Krupp et al. 1986; Krupp and Seward 1987). Holocene pumice of the Taupo Subgroup and hydrothermal eruption breccia cover much of the surface of the thermal area (Healy 1965; Vucetich and Pullar 1973; Collar and Browne 1985). Hot springs discharge predominantly acid-sulphate-chloride waters (pH of 2-4) (Ellis and Wilson 1961; Jones et al. 2000; Teece 2000; Mountain et al. 2003). The most prominent surface features are the acidic (pH ~2.3) Lake Rotokawa of 0.6 km^2 and the main thermal area directly to the north (Forsyth 1977; Krupp et al. 1986; Krupp and Seward 1987). On the northeast-

Figure 2. Overview of the study site with view to the south. Parariki Stream to the left is 2 m wide and flowing north.

ern margin of Lake Rotokawa, hot spring activity occurs in a terrace called "Sinter Flat" (Krupp et al. 1986; Krupp and Seward 1987). Several thin siliceous deposits and stromatolitic growth features have been described from this terrace (e.g., Krupp et al. 1986; Krupp and Seward 1987; Jones et al. 2000; Teece 2000; Mountain et al. 2003).

Lake Rotokawa drains via Parariki Stream in a northeast direction from the east side of the lake into the Waikato River (Figure 1.2). Numerous hot springs situated on the stream banks discharge silica-rich, acid-sulphate-chloride waters along the southern part of the stream (Grange 1937; Forsyth 1977; Krupp and Seward 1987; Teece 2000).

The study site is situated on a pumiceous floodplain (Figure 2), located primarily alongside the western bank of the Parariki Stream, ~1 km northeast of Lake Rotokawa (Figure 1.2, red arrow). This floodplain is ~30 m long, up to 7 m

wide and separated from the stream by a series of riffles, composed of well sorted coarse pumiceous alluvium (Figure 3). Through most of the year in 2004, the stream was confined to its channel and did not infiltrate the floodplain. During summer, thermal water levels were often lower than during winter. Hot spring vents at this site discharge mostly clear acid-sulphate-chloride waters (Table 1) ranging from 91 to 40°C with an average pH of ~2.2 (Figure 4). Teece (2000) determined that silica in the Parariki discharge waters is predominantly monomeric. The spring water discharging into the Parariki Stream and the study site contain about 300 mg kg^{-1} SiO$_2$ (Table 1). They are thus very close to saturation with respect to amorphous silica but oversaturated in silica with respect to opal-CT, opal-C and quartz (cf. Fournier, 1985; Dove and Rimstidt, 1994). The relatively high silica contents are a legacy of the >320°C equilibration temperatures in the geothermal reservoir (Krupp et al. 1986; Krupp and Seward 1987), with silica derived from depth, rather than being leached from the surface rocks, as is the case in many acid-sulphate areas (cf. White et al. 1956; Rodgers et al. 2002, 2004). For this reason, deposits forming directly from these silica-rich waters are interpreted to be silica sinter, rather than silica residue (Rodgers et al. 2004).

At the study site, four main types of siliceous sinter deposits were discerned (Figure 3). They are defined herein as four distinct sedimentary microfacies based on temperature and hydrodynamics of surrounding thermal water, the geometry, size and texture of the sinters, as well as their associated microbiota.

MICROFACIES CHARACTERISTICS AND SINTER PROPERTIES

Microfacies 1 – Cup- to Ridge-Shaped Sinter

Microfacies 1 (Figure 3) sinter forms in slightly turbulent waters with high emissions of steam, and water temperatures ranging from 91°C at some vents to 64°C in the associated discharge channels (Figure 4.1). The water turbulence is caused by the

Table 1 Composition, temperature, and pH values of representative sampling localities at 11 and 21 (see Figure 4). Concentrations are in mg kg^{-1}.

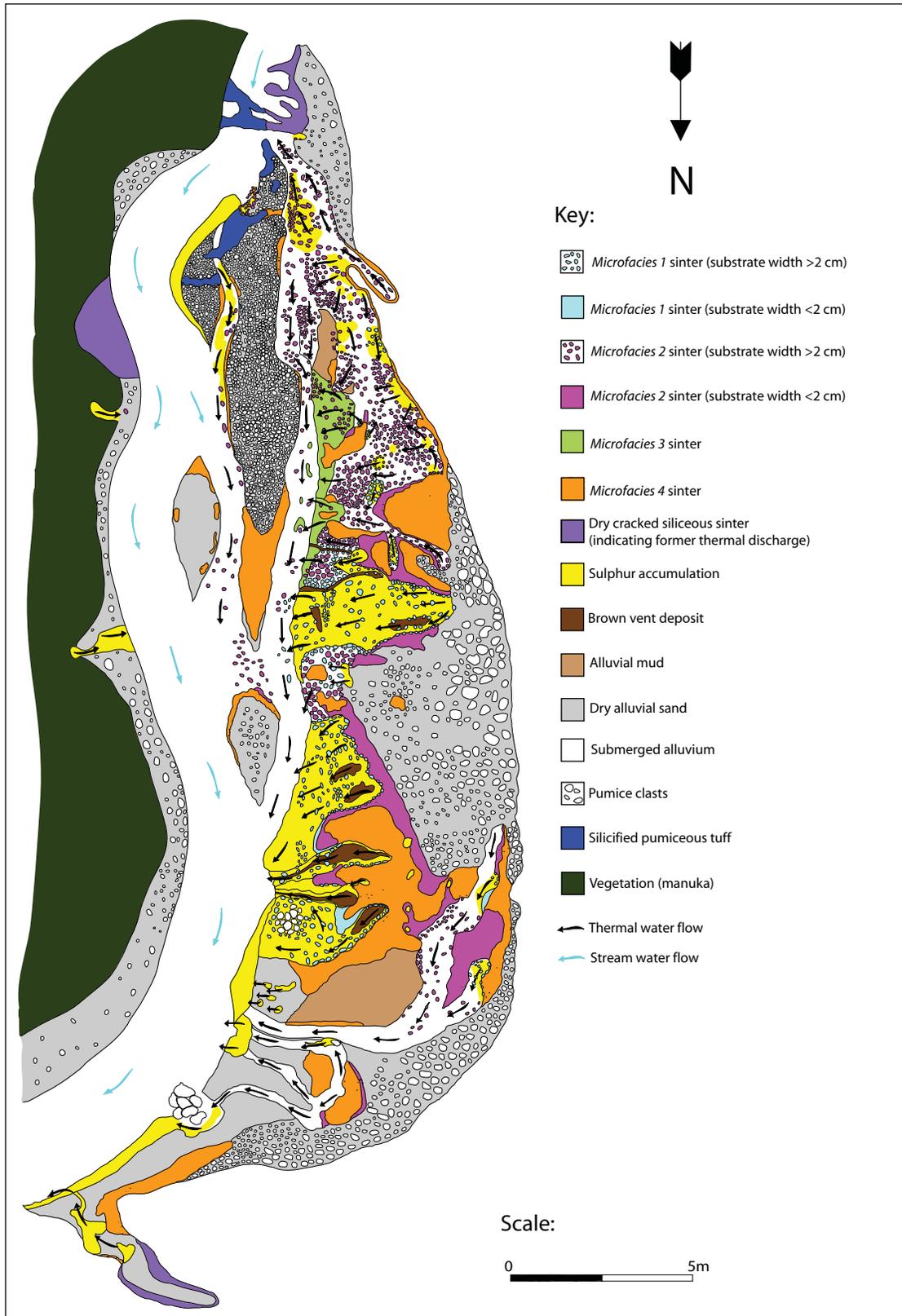| Location	T (°C)	pH	Li	Na	K	Mg	Ca	B	Al	Fe	SiO$_2$	As	Cl	HCO$_3$	H$_2$S	SO$_4$
11	72	2.1	2.8	333	31	6	33	17.1	39	15.7	297	0.63	448	25	0.47	1340
21	84.6	2.26	2.5	313	32	6.9	34	15.5	28	15.8	302	0.51	393	26	3.4	1282

Figure 3. Map of the study site showing the spatial distribution of the four distinct sedimentary microfacies of siliceous sinter formation. Also shown are thermal and stream water flow directions, the distribution of alluvium, sulphur accumulations, outcrops of silicified pumice tuff, and vegetation.

ebullient discharge from nearby vents that produces pulses of thermal water (typically 85°C) washing onto the siliceous sinters. Neither splash nor spray was observed around these deposits. However, water level changes were recorded in this microfacies (Figure 4.1). Sinter forms subaerially on pumice clasts and pine cones that act as substrates above water level (Figure 5). Sinter accretion rates were fastest at this microfacies. An average of 0.24 g silica accumulated on glass slides over 67 days in this environment (Figure 4). It is unknown if *Microfacies 1* sinter accreted at a uniform rate or not.

XRPD analyses of sinters from this and all other microfacies of this study site showed that they are composed almost entirely of opal-A, with minor traces of detrital quartz and/or feldspar (for full width at half maximum intensity (FWHM) values and density/porosity data, see Rodgers et al. 2004). DTA of sinters from this study also gave identical traces characteristic of opal-A, with no indications of clay content (cf. Herdianita et al. 2000a). TGA of these sinters indicated weight loss of approximately 5 to 6% resulting from opal-A dehydration (cf. Herdianita et al. 2000b; Handley et al. 2005).

Microfacies 1 sinter is vitreous, light grey in colour, and usually cup- or ridge-shaped with minute microspicules (0.5 cm high) visible on the uppermost sides of the rim or within cavities (Figure 5.2). The sinter surfaces have multiple, thin layers of silica with an irregular texture, and are composed of gnarled, broken, and isolated surface remnants (Figure 5.4). This irregular texture is gradational, occurring predominantly in the lowermost portions of the sinter, close to the air-water interface. Vertical sections through the sinters exhibit alternating series of light brown and light grey laminae (Figure 5.5). The laminae range from <2 to 50 µm in thickness and alternate between brown to dark brown and clear, translucent silica (Figure 5.6). No evidence for the presence of microorganisms or any mineral-microbe association was observed in thin-section. Laminae in the lower portions of the sinters are relatively flat, but become progressively more convex upwards. On and within these layers, conical microspicules may be present, but in a relatively lower frequency than in *Microfacies 2* (see below). Under SEM, vertical sections appeared vitreous and massive, without any conspicuous laminae. Prokaryote-sized microorganisms were only rarely observed in these sections.

At the Parariki site, sinter morphology is affected by the subaerially exposed substrate dimensions. Substrates that are relatively wider and higher above water exhibit limited siliceous coating. This coating is confined to the outer fringes of the substrates, resulting in the formation of cup-shaped deposits (Figure 5.2). On substrates that are low-lying and less aerially extensive, silica deposited across the substrate and a ridge-shaped deposit arises (Figure 5.3).

Large areas of *Microfacies 1* sinter surfaces are covered by irregularly lobed, coccoidal microorganisms (1-1.5 µm in diameter) (Figure 6.1). These microbes are linked to one another through a meshwork of mucosal to filamentous extracellular polymeric substances (EPS). Such microbe-EPS assemblages are known as biofilms (cf. Cady and Farmer 1996; Handley et al. 2005). Biofilms in the upper- and inner-most portions of the Parariki sinters typically assumed the shapes of isolated, conical cell clusters (Figure 6.2). Some of these clusters became progressively encrusted by nanospheres of silica (<250 nm in diameter) and eventually recolonised by a new succession of microbes (Figure 6.3-6.4). Note that individual nanospheres attached directly to the cells and the associated EPS, thereby starting the process of silicification. Cells that appeared free from these silica spheres may be tentatively regarded as unsilicified.

The continuous interplay between microcolony formation, silicification, and recolonisation appears to have formed vertically upright, pillar-like microspicules (Figure 7). The upper surfaces of these spicules displayed a knobby morphology (typically 1-2 µm in diameter) of similar dimensions to nearby coccoidal cells (Figure 7.3). Thus we infer that individual knobs formed by the silicification of these microbial cells. The knobby texture was only observed on spicules of *Microfacies 1*, where it coincided with the presence of coccoidal microbial cells. We did not observe this texture on spicules from other microfacies where bacilli (rod-shapes) predominate (see below).

The irregularly lobed cocci are regarded as microbial cells and not as abiogenic crystals, since they are highly irregular in shape, often associated with copious EPS (Figure 6) and are very similar in morphology under SEM to cultured archaeal thermoacidophiles (e.g., Chen et al. 2005, figure 5A). Indeed, 16S rRNA genes extracted from *Microfacies 1* sinter is related to known thermoacidophiles that also have irregularly lobed sphere shapes (e.g., Thermoplasmatales; Schinteie 2005).
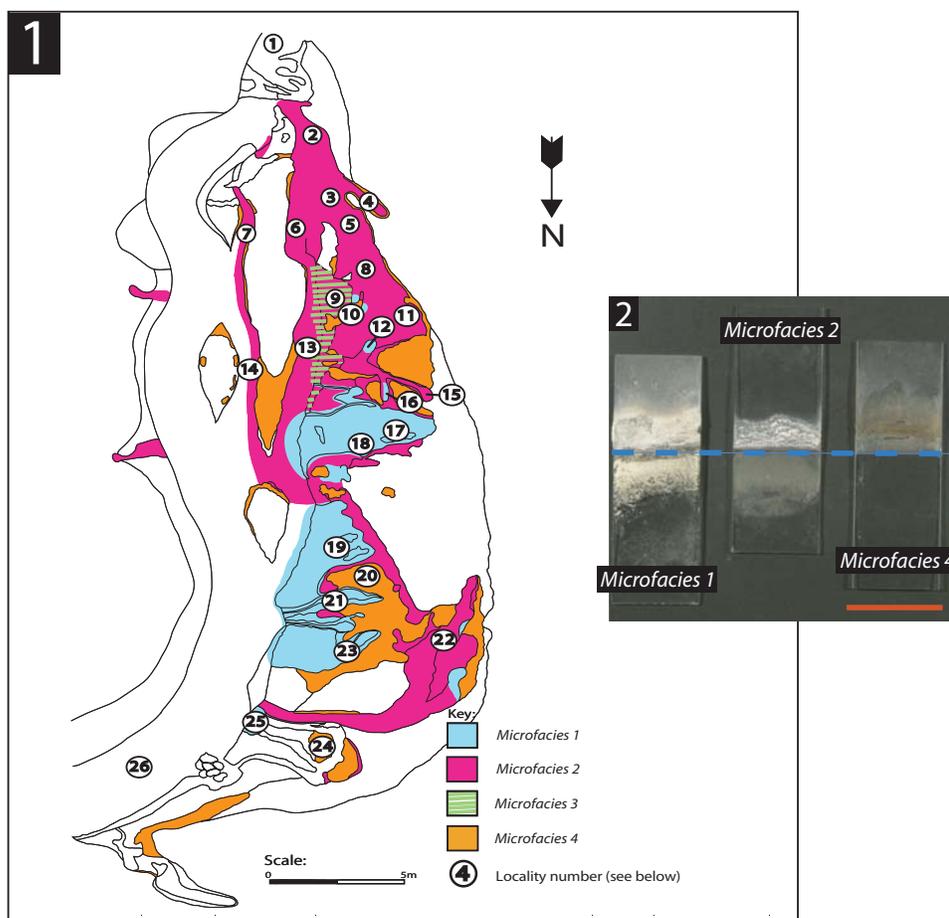
Figure 4. Characteristics of discharged thermal water from each microfacies. **4.1** Map of the study site showing approximate microfacies locations. Numbers refer to localities were measurements were taken (see Figure 4.3). **4.2** Representative examples of glass slides with subaerially accreted silica after 67 days. Differences between slides indicate different rates of subaerial silica accretion. Dashed blue line marks average water level. Note the relatively large subaqueous sulphur accumulation in Microfacies 1. A yellow-light brown substance (sulphur? and/or organics?) accumulated subaqueously in Microfacies 2. Bar represents ~3 cm. Silica accretion rates were unable to be measured for Microfacies 3.

SEM examination revealed that silica deposited predominantly as spheres of opal-A that are primarily <10 nm to 50 nm in diameter. However, spheres can grow up to 500 nm in diameter through the aggregation of smaller spheres. Two types of sphere shapes were observed: (1) freshly deposited, round equidimensional spheres; and (2) more poorly defined spheres with interparticle "necks" (Figure 8.1-8.2) (cf. Iler 1979, figure 3.24). The poorly defined sphere shape-texture was pervasive on *Microfacies 1* sinter. Associations between this texture and microorganisms were not observed under SEM. In addition to silica, well developed crystals of gypsum, barite, and sulphur were present. No clay minerals were observed

anywhere upon or within sinter from this or any other microfacies at the Parariki site. The absence of clay minerals is in contrast to acid-derived sinters and residues reported elsewhere in New Zealand (Jones et al. 2000; Rodgers et al. 2002).

At the microscale, the surfaces of the lower portions of *Microfacies 1* sinter are irregular and uneven. Anastomosing ridges, nodules, and associated cavities are common. Incipient ridges appear as surface irregularities that are bounded by small cavities (Figure 8.3-8.4). Within these cavities, nodules formed that eventually become mushroom-shaped, producing a neck-like structure (Figure 8.4-8.6). While incipient nodules are sur-

Figure 4 (continued) 4.3 Temperature, pH, water level changes and silica accretion measurements. N.R. = not recorded. No significant water temperature changes were observed between seasons.

Locality number	Microfacies	Water temperature (summer/winter) (°C)	Water level (summer/winter) (mm)	Water pH	Silica accumulation over 67 days (g)
1	Stream	30.8/17	150/159	2.03	N.R.
2	2	49	12/14	2.3	0.1287
3	2	55	N.R.	2.25	N.R.
4	2	58	20/23	2.14	N.R.
5	2	57.9	8/12	2.23	N.R.
6	2	55	12/18	2.23	0.1289
7	2	54.6	12/15	N.R.	N.R.
8	2	58	12/16	2.3	0.1281
9	2 and 3	59.8	6/10	2.13	N.R.
10	4	45	No change	2.24	0.0092
11	2	85	10/12	2.10	0.0802
12	1	64.2	10/14	2.13	N.R.
13	2	54	10/19	2.12	N.R.
14	2	38.8	130/136	N.R.	N.R.
15	2	63	5/8	2.24	N.R.
16	1	63.9	6/10	N.R.	N.R.
17	1	83.2	N.R.	2.28	0.2752
18	1	76.1	25/28	N.R.	N.R.
19	1	78.2	20/25	N.R.	0.2036
20	4	67	No change	N.R.	0.0098
21	1	84.6	N.R.	2.26	N.R.
22	2	59.4	18/20	2.23	N.R.
23	1	78.1	21/25	2.27	N.R.
24	4	52	No change	2.22	N.R.
25	1	91	N.R.	N.R.	N.R.
26	Stream	33.2/20.9	120/130	N.R.	N.R.

rounded by small cavities, taller nodules are associated with deeper cavities and larger ridges.

The lower portions of *Microfacies 1* sinters exhibit isolated patches of surficial silica sheets (Figure 9.1). These sheets appeared to have become progressively contracted and diminished, particularly around necks (Figure 9.2), so as to leave behind isolated remnants of a formerly continuous surface. The patches are bound by anastomosing ridges (Figure 9.3) that are larger towards the outer fringes of these isolated patches (Figure 9.4). Figure 9.1-9.4 show the surface of silica grown onto a glass slide for one month in a *Microfacies 1* setting. Surfaces of natural *Microfacies 1* sinter show even more extreme forms of isolated remnants (Figure 9.5-9.6), presumably because they have been in this environment for much longer than the slides. These remnants contain concentric laminae, mirroring the topography of the underlying layers, as well as ridges, which are larger on the fringes.

Microfacies 2 – Spiculose Sinter

Microfacies 2 (Figure 3) is characterised by quiescent thermal water discharge. Steam emission is also minor, while water temperatures range from ~85°C to ~30°C (Figure 4.1). As in *Microfacies 1*, neither splash nor spray was observed around these deposits. *Microfacies 2* sinter forms subaerially on pumice clasts, wood, pine cones, and dead insects (Figure 10). Water level changes have also been observed in this microfacies (Figure 4.1). Steam condensate keeps the sinters moist. Silica accretion rates are slower than those in *Microfacies 1*; an average of 0.12 g silica accreted on the slides over 67 days (Figure 4).

The outer and lower portions of *Microfacies 2* sinters are usually covered by a ubiquitous green microbial mat (Figure 10). Transmission electron microscopy (TEM) and rRNA gene analysis indicates that these mats are primarily composed of coccoidal algal cells related to the rhodophyte taxon Cyanidiophyceae (*Cyanidium* and *Galdieria*;
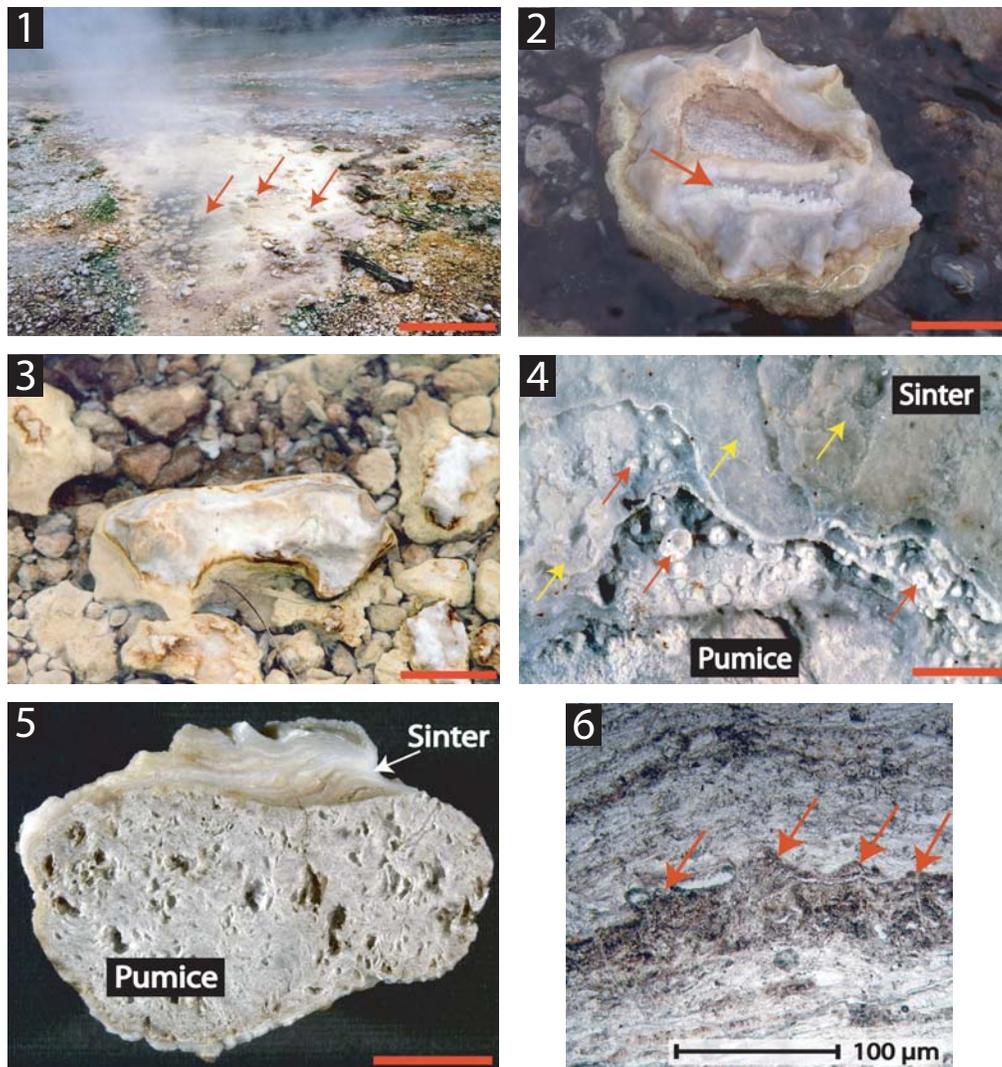
Figure 5. Field occurrences and hand specimens of *Microfacies 1* sinter. (1) Overview of *Microfacies 1* represented by a sulphur-emitting vents (84°C) around which subaerial sinter forms (red arrows). White-grey and orange deposits to the left and right belong to *Microfacies 2* and *4*, respectively. Green microbial mats form where water cools to <52.5°C. Note copious steam emission around sulphur discharging vent. Bar represents ~1.5 m. (2) Cup-shaped sinter (grey rim) depositing on the surface of a pumice clast. Spicules formed within a cavity on the uppermost side of the rim (red arrow). Bar represents 3 cm. (3) Ridge-shaped sinter on a pumice clast. Bar represents 3.5 cm. (4) Close-up of the lower portion of a *Microfacies 1* sinter deposit. Multiple flat siliceous layers (yellow arrows) exhibit an irregular, gnarled surface texture. Isolated patches of silica (red arrows) also occur. (5) Vertical section through sinter and pumice substratum. Note the alternating light brown and light grey laminae. (6) Thin-section micrograph showing microspicules (red arrows) along the length of a brown lamina. Laminae become increasingly more convex upwards.

Schinteie 2005). The mats occur where temperatures are between 52.5 and 30°C. On sinter, the mats are at their thickest (1 mm) at ~ 45°C. On the uppermost portions of the sinters, where temperatures are often slightly cooler and less exposed to thermal water, the mats become faint and disappear.

The sinters are white to vitreous in colour, and typified by significant spicular growth (Figure 10). The spicules are needle-like to conical in shape, 1 to 3 mm wide, and from <1 mm to ~1 cm long. Spicules are densely packed, accrete perpendicular to the substratum, and become progressively smaller outward towards the water. A rim forms where spicules progressively link laterally with each other through a continuous deposition of silica (Figure 10.2 and 10.5; cf. Handley 2004). Vertical sections through these sinters revealed alternating light and dark laminae (Figure 10.6).
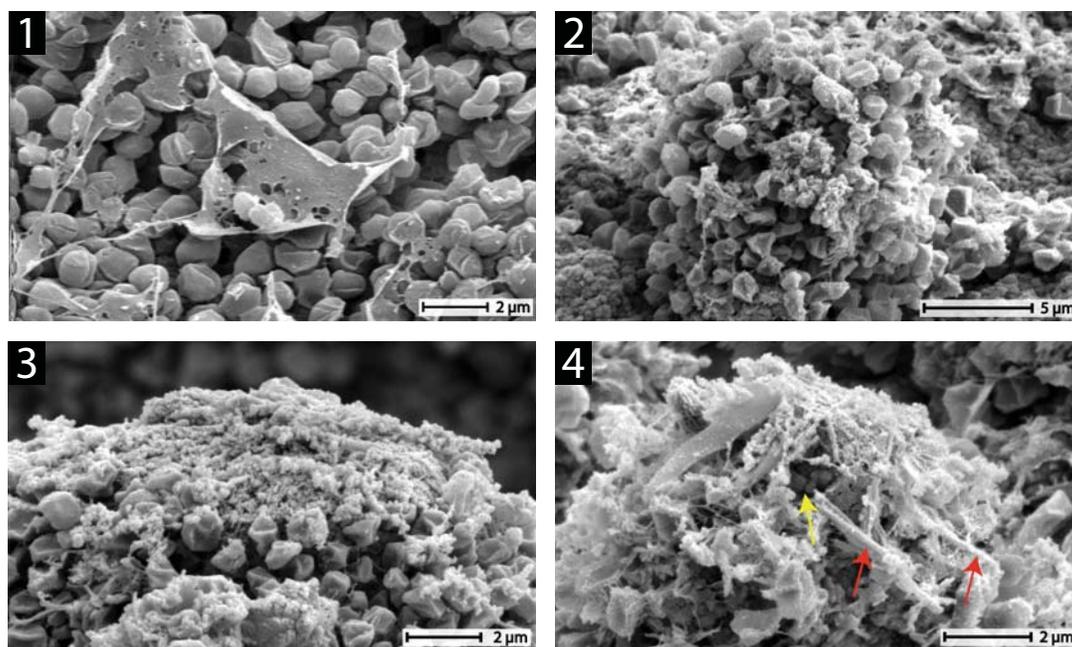
Figure 6. Microbial colonisation and microcolony formation associated with *Microfacies 1* sinter. (1) Irregularly lobed, coccoidal cells, and associated EPS. (2) Close-up of a conical microcolony. (3) Preferential silicification on the uppermost portion of a microcolony. (4) Colonisation of a silica substratum (yellow arrow) by a succession of partially silicified biofilm. Red arrows indicate acicular, aluminum, and oxygen-rich minerals (as determined by EDS) of unknown phase.

The laminae alternate among laterally continuous green, brown, and translucent silica (Figure 11.1). As in *Microfacies 1*, laminae in the lower sinter portions are relatively flat but become progressively convex upwards (Figure 11.2), culminating in spicules composed of parabolic laminae. The fate of incipient spicules varied over time; some became reinforced by the deposition of successive laminae, whereas others were smothered or dampened by the lamination process (Figure 11.3 and 11.4). Overall, the relief of the sinters increased over time, with surfaces characterised by abundant, erect, and free-standing spicular structures with parabolic laminae. Numerous spicules also exhibit branching and small (~0.5 mm) projections with internal convex laminae.

The green laminae observed in thin section (Figure 11.5) are composed of spheres that are similar in size (2-10 µm) and appearance to the coccoidal cells present in the green biomats (Figure 11.6). These cells are restricted to the lower and middle portions of *Microfacies 2* sinter, corresponding to the distribution of the living green mats. Diatom tests occur throughout the sinter.

As in *Microfacies 1*, sinter morphology also is controlled by substrate shape and dimensions. Subaerial substrate portions that are relatively wider and higher above water exhibit less siliceous encrustation relative to substrate size than deposits that are low-lying and have smaller widths. While wider substrates display sinter with cup-shaped morphologies (Figure 10.2), smaller substrates are covered in spicules that coat much of the subaerial portions (Figure 10.3). The extent of siliceous covering in *Microfacies 2* is less than that of comparable substrate sizes and shapes in *Microfacies 1*, where relatively higher energy conditions occur.

Bacilli (i.e., rod-shaped microorganisms) (1-2.3 µm long) dominate the sinter biota of this microfacies (Figure 12.1). The microbes are usually associated with a meshwork of EPS that includes both fibrous and mucosal textures. These biofilms became progressively silicified by coalesced to partially coalesced opal-A nanospheres (100 nm) and microspheres (250 nm) (Figure 12.2). Eventually, the films were completely obliterated by the deposition of overlying spheres.

The bacilli also tended to form clumps of microcolonies which grew perpendicular to the silica surface and were associated with a network of EPS (Figure 12.3). In places, diatom tests provided areas of positive relief onto which new clusters of bacilli aggregated. As in *Microfacies 1*, such micro-
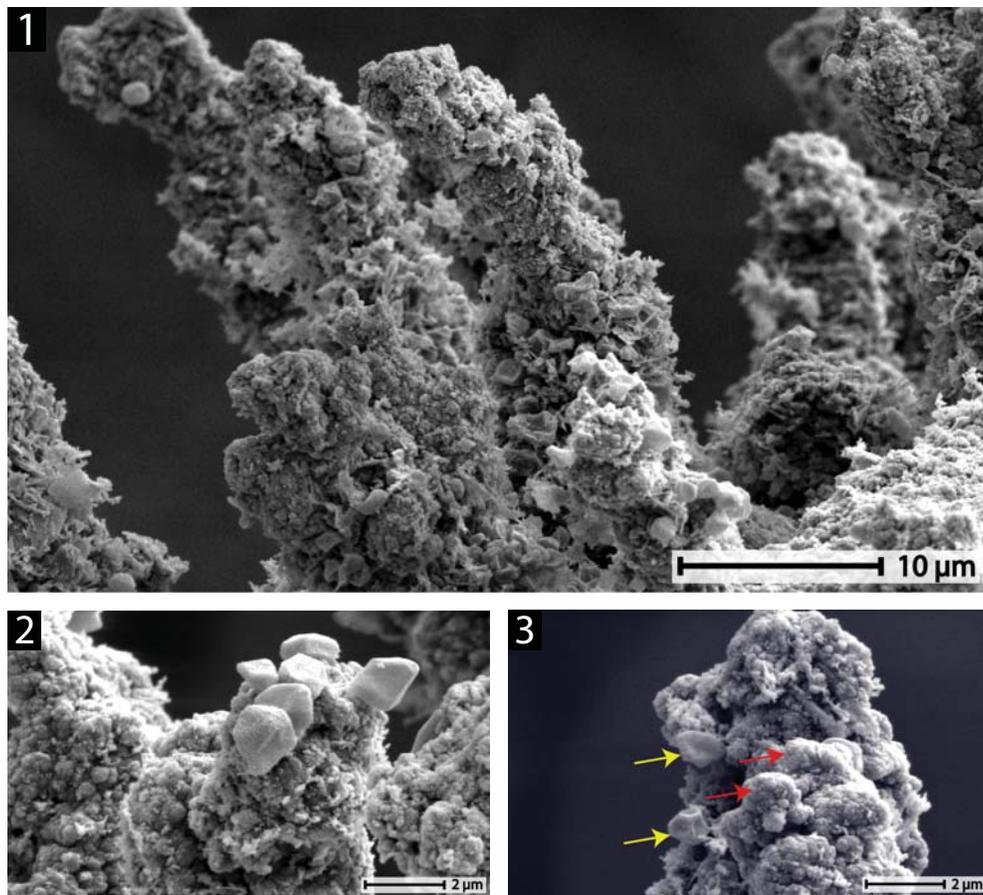
Figure 7. Formation of microspicular structures on *Microfacies 1* sinter. (1) Upright microspicules at various stages of growth and covered with microbial cells. (2) Cluster of cells attached to the top of a microspicule. (3) Knobby texture on the uppermost portion of a microspicule with individual knobs (red arrows) equal in size to unsilicified cells (yellow arrows).

colonies became silicified, forming areas of positive relief (Figure 12.4). This consistent interplay between bacterial colonisation and silicification also resulted in the formation of microspicules. The possible outlines of bacilli inside spicules are preserved (Figure 12.6). The occurrence of vertically upright microcolonies in *Microfacies 2* is more widespread than in *Microfacies 1*.

Pennate diatoms, predominantly *Pinnularia acoricola* Hustedt and *P. champmaniana* Foged, constitute a major component of the sinter biota (Schinteie 2005; cf. Foged 1979; Cassie 1989; Cassie and Cooper 1989). These diatoms preferentially occupied areas of low microrelief, such as crevices and cracks, as well as overlying areas of positive relief (Figure 13.1-13.3). The mode of attachment for these benthic diatoms is adnate, or closely appressed to the substratum, with the entire valve attached to a substrate by a coating of EPS (Figure 13.4). In open areas of the deposits that do not offer sheltering by surrounding sinter,

diatom tests were often found fractured and amassed into clumps (Figure 13.5). Diatom assemblages may eventually become part of the sinter deposit, starting with the precipitation of silica spheres onto the tests, which eventually result in their complete cementation (Figure 13.6) (cf. Jones et al. 2000; Campbell et al. 2004). In this and in other microfacies of the Parariki site, early silicification occurs preferentially on the edges of diatom tests, EPS sheets, and fibres.

The green algal-dominated mats present on the lower surfaces and in thin section of *Microfacies 2* sinters are largely composed of colonies of spherical cells (2-10 µm in diameter) that are covered in membranous sheets (Figure 14.1). The cell surfaces of these mats can become encrusted and incorporated into lower portions of the sinter (Figure 14.2-14.4; cf. Figure 11.5-11.6). Vertical sections through these portions exhibit numerous horizontal laminae (~100-180 µm thick) of dense, vitreous sinter, alternating with layers (~80-120 µm
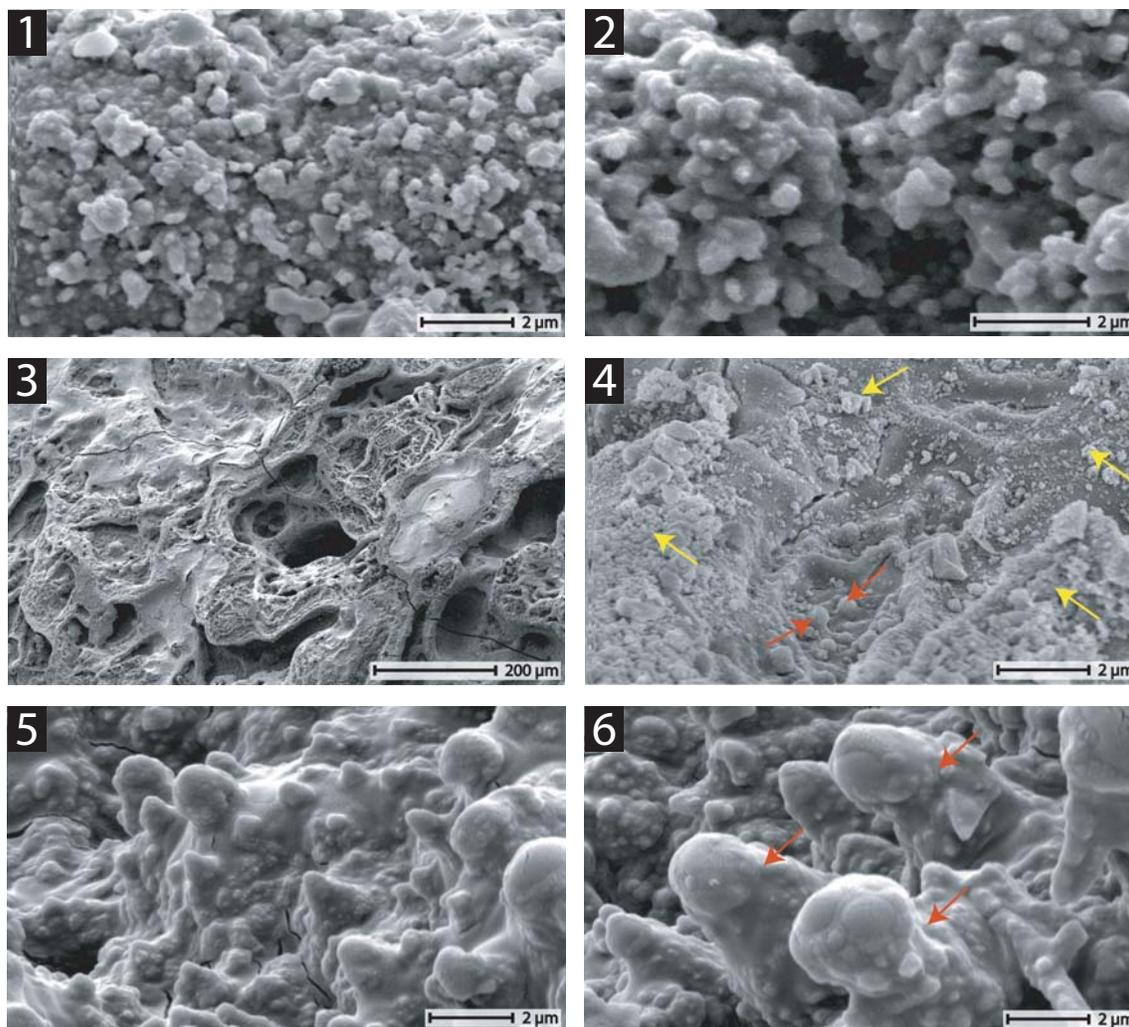
Figure 8. Formation of irregular silica surface textures on *Microfacies 1* sinter. (1) Clusters of coalesced silica spheres. (2) Close-up of (1) showing ill-defined outlines. (3) Anastomosing ridges and cavities at various stages of formation. (4) Incipient occurrence of ridges, associated cavities, and nodules (red arrows). Note broad deposition of secondarily deposited silica spheres (yellow arrows). (5) Early-stage occurrence of nodules, acquiring a cone to round shaped surface. (6) Late-stage occurrences of nodules, exhibiting necking (red arrows).

thick) dominated by silicified cells that are equal in size to cells of the living green mats (Figure 14.5). Several silicified cells also exhibited endospores (i.e., internal division of parental algal cells). In some instances, cellular impressions were preserved (Figure 14.6). The boundary between the predominantly abiotic and biotic layers is sharp and planar, showing that cells of the green mats initially colonised a flat surface before becoming silicified (Figure 14.4).

Unlike sinter surfaces of *Microfacies 1*, those from *Microfacies 2-4* are generally not irregular in appearance. Ridges, nodules, isolated remnants, or associated cavities were rarely observed. Furthermore, their opal-A spheres (also <10 nm to 50 nm in diameter) tended to be more spherical in shape.

Microfacies 3 – Parallel Laminated Sinter

Microfacies 3 sinter (Figure 3) is confined to the southern portion of the study site, which slopes at ~10° E from the horizontal. Although these deposits are usually submerged under flowing thermal water (Figure 15), the water level in this area is lower (~6-10 mm) than that flowing on flatter areas (>10 mm) elsewhere at the site (Figure 4.1). Therefore, this microfacies is affected by changing water levels, completely exposing the sinters to the air in times of lower water levels. Water temperatures range from ~60-54°C (Figure 4.1).
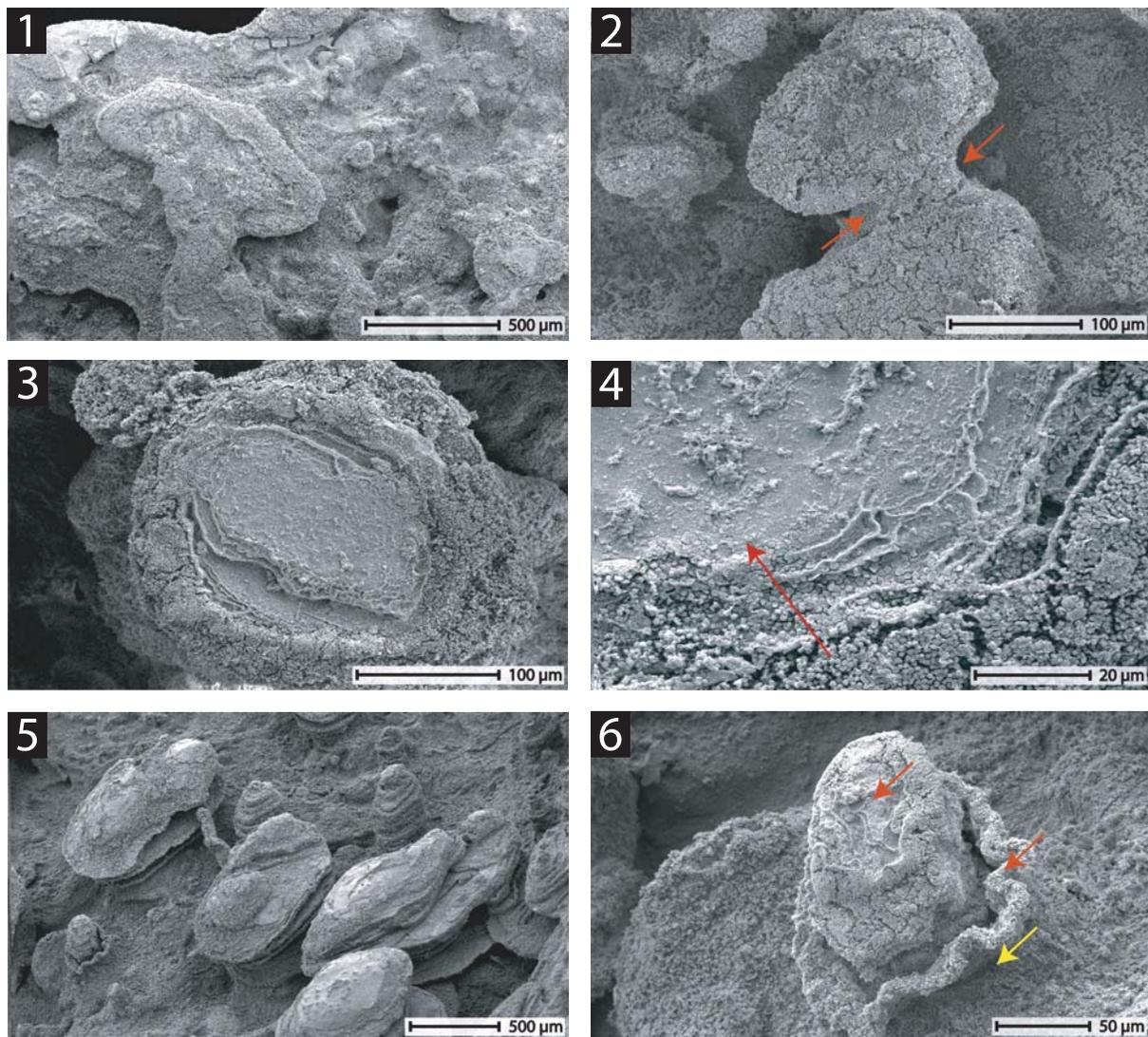
Figure 9. Isolated patches on the lower portions of *Microfacies 1* sinter. (1) Overview of a sinter surface grown on a glass slide for one month and showing isolated patches of surficial layers. (2) Necking of isolated patches (red arrows). (3) Isolated patches exhibiting ridges around their sides. (4) Close-up of (3) showing ridges becoming progressively smaller inwards towards the centre of the isolated patch (red arrow). (5) Isolated remnants exhibiting concentric laminae. (6) Remnant island exhibiting necking (yellow arrow) and numerous ridges (red arrows) that increase in size towards the outer fringes.

Sinter from this environment is flat and parallel-laminated (Figure 15.1). Surfaces are irregular and even rippled in places, which appears to be due to the patchy nature of ongoing silica deposition (Figure 15.2). During lower water levels, small, isolated puddles of thermal water occur in the irregular surface crevices of the sinters. Continuous patchy silica deposition on these sinters results in silica rims (Figure 15.3) that eventually grow into cup-like deposits like those of *Microfacies 2* (Figure 15.4). Indeed, pumice clasts that rest partially submerged in these waters and on top of the planar sinter deposits act as substrates for *Microfacies 2* sinters (Figure 15.1). Due to the thinness of *Microfacies 3* and *4* sinter (~<3 mm and 2 mm, respectively), no thin sections were made of these two deposit types. Because of difficulties in permanently placing glass slides horizontally, silica accretion rate measurements were also not conducted for this microfacies. Any silica that deposits on vertically oriented slides would have represented *Microfacies 2* conditions.

SEM revealed that the upper surfaces of *Microfacies 3* sinters are colonised by bacilli (1-8
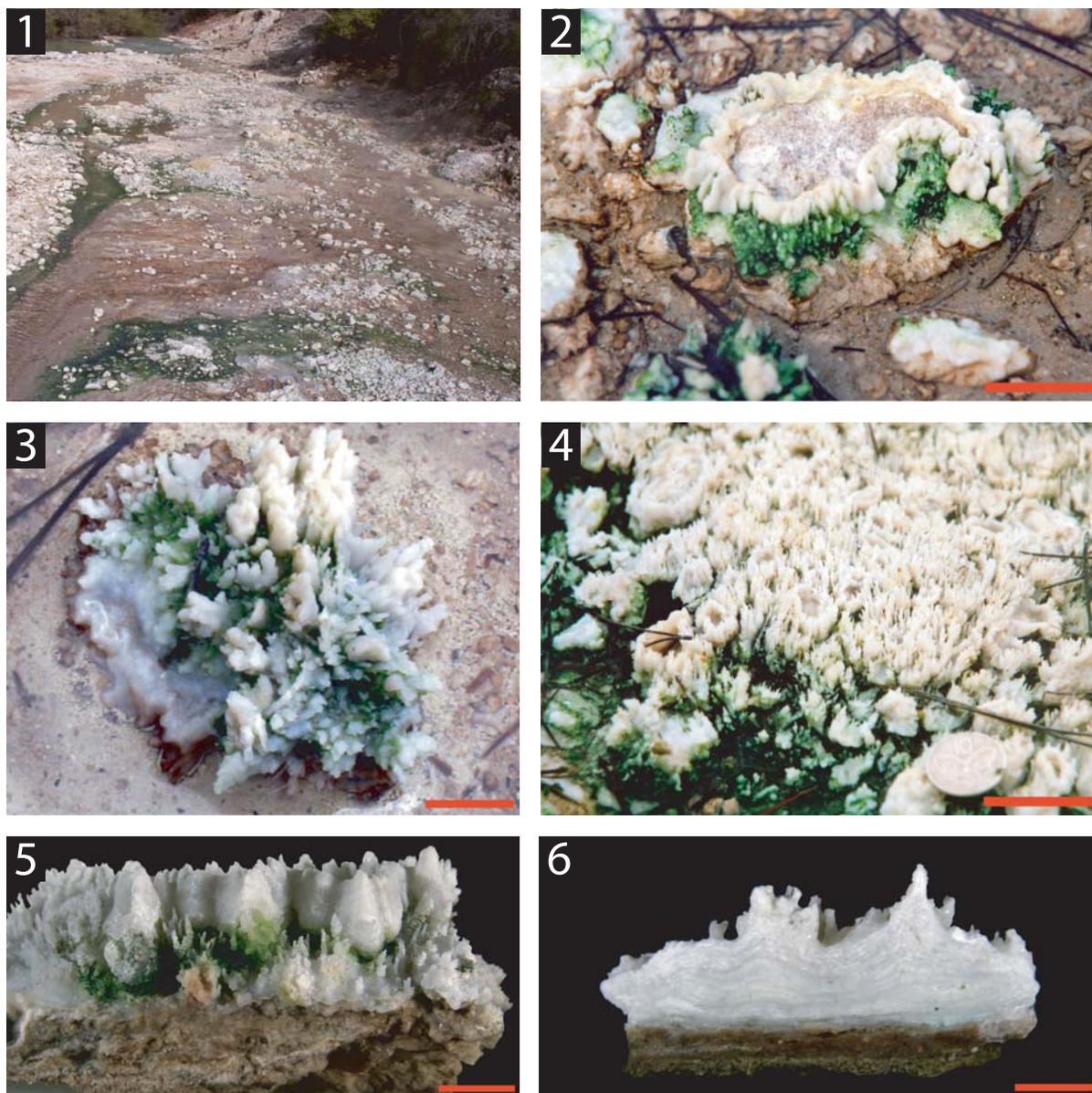
Figure 10. Field occurrences and hand specimens of *Microfacies 2* sinter. (1) Overview of *Microfacies 2* with sinters (white deposits) surrounded by relatively quiescent thermal water. A green microbial mat (algal) covers portions that are 52.5°C. Photo width is ~5 m. (2) Cup-shaped siliceous sinter (white rim and green/white spicules) depositing on the upper surface of a pumice clast. Bar represents 4 cm. (3) Spiculose deposit covering entire substrate surface. Bar represents 1.5 cm. (4) Cup-shaped and spiculose deposits forming in areas where thermal water flow is confined to small spaces between densely clustered substrates. Coin at the lower right is 2 cm wide. Bar represents 2.5 cm. (5) Side-on view of sinter showing a rim along inner portions of the deposit, while the outer portions are covered by vertical spicules. (6) Vertical section through sinter showing a white deposit with fine laminae. Sinter rests on a silicified sandy substratum (brown). Bar represents 1 cm.

µm long) (Figure 16.1). Silicification of these microbes was patchy, with nanospheres (<100 nm) of silica precipitating onto the uppermost portions of cells, whereas those beneath were unsilicified (Figure 16.2). Vertical sections of the sinters reveal silica with a predominantly massive, vitreous texture (Figure 16.3). Cavities, cemented diatoms, and spherical cells (2-10 µm in diameter), resembling those from the green living mats, are the only discernable features in these sections (Figure 16.3-16.4).
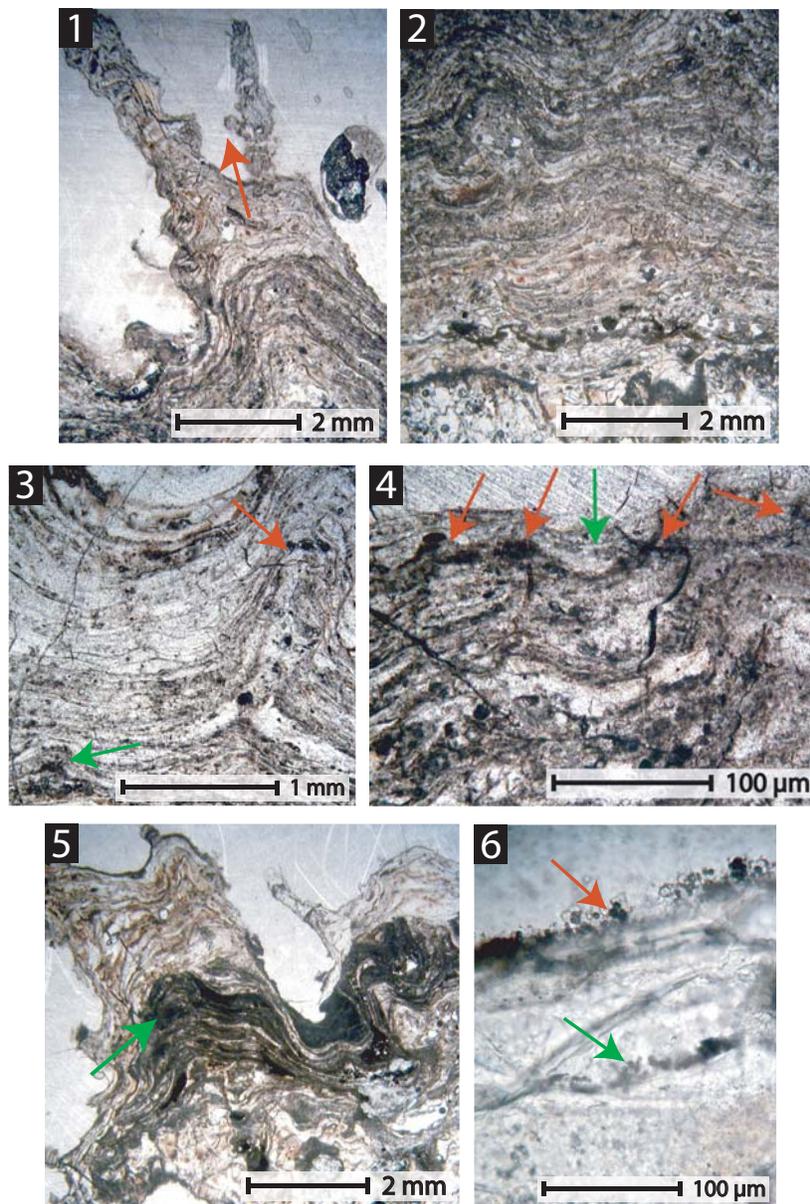
Figure 11. Thin-section micrographs of *Microfacies 2* sinter. (1) Branching spicules exhibiting projections (red arrow) on their sides. (2) Close-up of sinter laminae that become increasingly convex upwards. (3) Reinforcement (red arrow) or dampening (green arrow) of microspicules by the deposition of successive laminae. (4) Conical microspicules (red arrows) growing on a lamina (cf. Figure 5.6). New layers of silica (green arrow) have subsequently covered the micro-spicules. (5) Overview of sinter displaying alternating laminae on the lower portions that are light brown and dark green in colour (green arrow). (6) Close-up of green laminae present on the sinter surface (red arrow) and incorporated into the sinter body (green arrow).

On vertical portions of the sinters that have subaerial rims (Figure 15.3-15.4), diatoms clustered together in large groups with the tips of their tests aligned perpendicular to the approximate air-water interface (Figure 16.5). These clusters also became progressively silicified and incorporated into the deposit (Figure 16.6).

Microfacies 4 – Thin Siliceous Rim Sinter

Sinters from *Microfacies 4* (Figure 3) are characterised by thin (~2 mm thick), orange, cup-like rims formed on small (<2 cm in diameter) pumice clasts that rest upon moist sandy substrates well above the outflow channels (Figure 17.1-17.3). The deposits can reach heights of 1-6 mm, with rare or
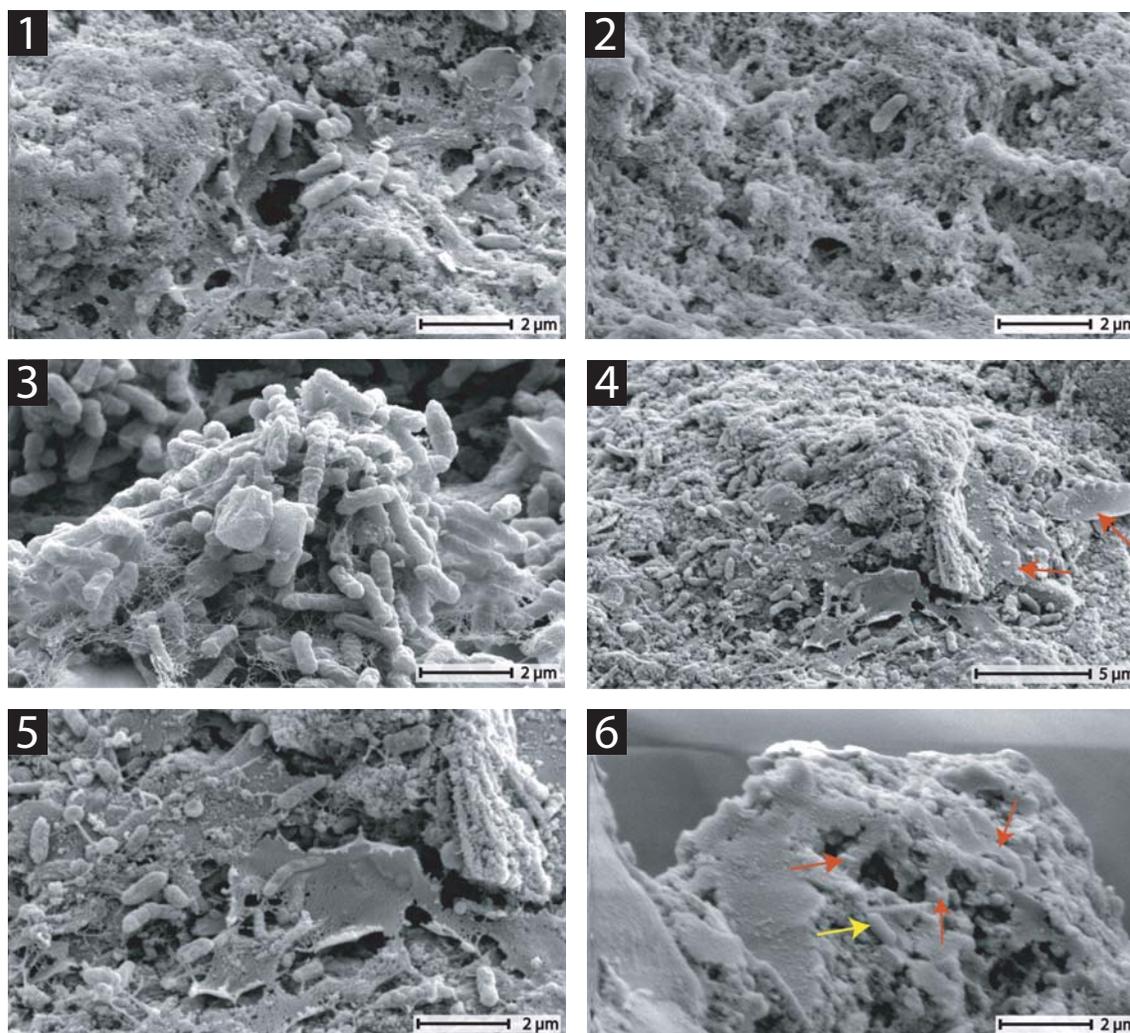
Figure 12. Microbial colonisation and microcolony formation on *Microfacies 2* sinter. (1) Bacilli associated with mucosal EPS. (2) Silicified mucosal EPS. (3) Conical microcolony formed predominantly by bacilli and fibrous EPS. (4) and (5) Formation of a conical microspicule, showing the close association between the presence of biofilms and silicification. Red arrows in (4) indicate diatom shells. (6) Cross-section through a microspicule, showing it to be composed of a network of rod-shapes (red arrows) that resemble bacilli. Yellow arrow points to a modern, unsilicified bacillus.

absent spicular textures. Vertical sections through the rims reveal thin internal laminae (~0.5 mm thick) that are convex rather than horizontal (Figure 17.4). The outer sides of these sinters are typically covered with green algal mats. Rarely, anastomosing ridges occur on the inner sides of the sinter rims (Figure 17.4).

Thermal water was not observed to wash, splash, or spray onto these deposits. Small holes dug into the sandy substrates revealed warm thermal pore water seeping upward through the sands (Figure 17.3). This water may derive from surrounding thermal discharges nearby, or from small unidentified vents underneath the sandy alluvium. The temperature of the seeping water was recorded to range from 45-67°C (Figure 4.1). Silica accretion rates in this microfacies averaged only 9.5×10^{-3} g over 67 days (Figure 4).

Sinter surfaces are covered by biofilms of diatoms (Figure 18.1-18.2), spherical microorganisms (2-6 µm in diameter) (Figure 18.3-18.4), and bacilli (1-2.3 µm long) (Figure 18.5). It is likely that the spherical cells are also algae, belonging to the green mats that cover the sinter rims on the margins of the deposits. Microbial silicification is likewise patchy, with some microbes completely covered in silica spheres, while others nearby are unsilicified. The bacilli also had the tendency to form vertically upright microcolonies, but were rarely observed to be silicified (Figure 18.5).
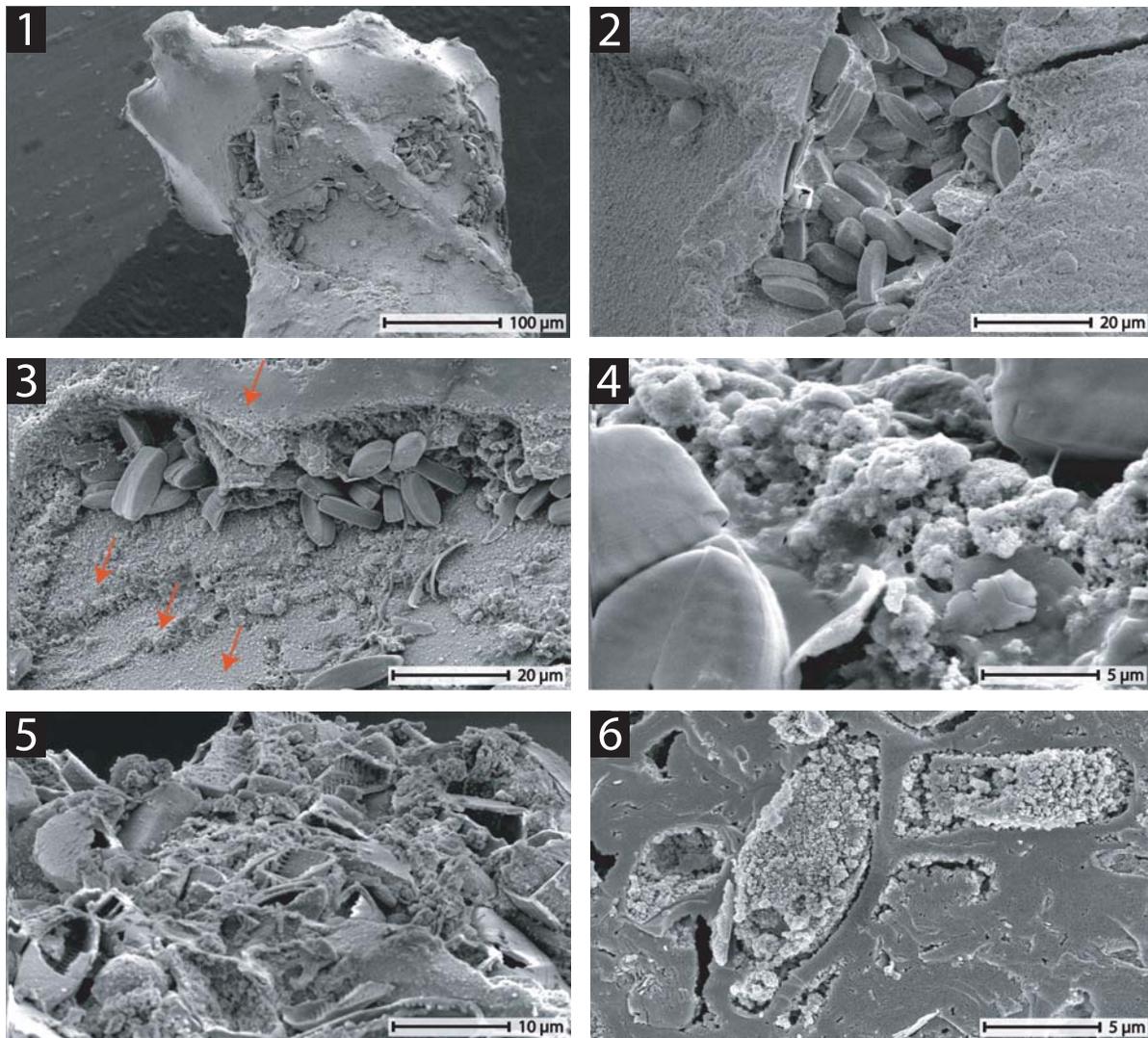
Figure 13. Lifestyle modes of diatom assemblages on *Microfacies 2* sinter. (1) Clusters of diatoms occupying numerous portions of a spicule. (2) Cluster of diatoms occupying a crevice on a spicule surface. (3) Diatoms wedged along layers of silica that act as surfaces of positive relief. Note the succession of silica layers that drape a spicule surface (red arrows), forming convex-upward layers similar to those observed in thin section (Figure 11.1). (4) Diatoms closely appressed to the surface by a coating of mucosal EPS. (5) Fractured diatom cells amassed together in an open area lacking shelter by surrounding sinter. (6) Cemented diatom cells incorporated into sinter.

SEM showed that vertical sections of these sinters comprise a massive, vitreous texture with no visible laminae. Silicified spherical cells (2-6 µm in diameter), often at the endospore stage, were commonly incorporated into the sinter (Figure 18.6). However, these organisms do not form layers as in *Microfacies 2*, but are scattered across the sinter.

DISCUSSION

This study assesses the effects of environmental variables on siliceous sinter deposition in the acidic waters of the Parariki study site. The restriction of different types of sinter morphologies, textures and associated microorganisms with respect to different microfacies shows that local environmental factors are of profound influence. Furthermore, a dynamic interplay between abiotic and biotic factors plays a major role in forming sinter textures. In the following discussion we evaluate the significance of different environmental variables (both abiotic and biotic) on the genesis of the Parariki sinters. Where appropriate, we also draw comparison with previous studies of acid-derived siliceous hot spring deposits.
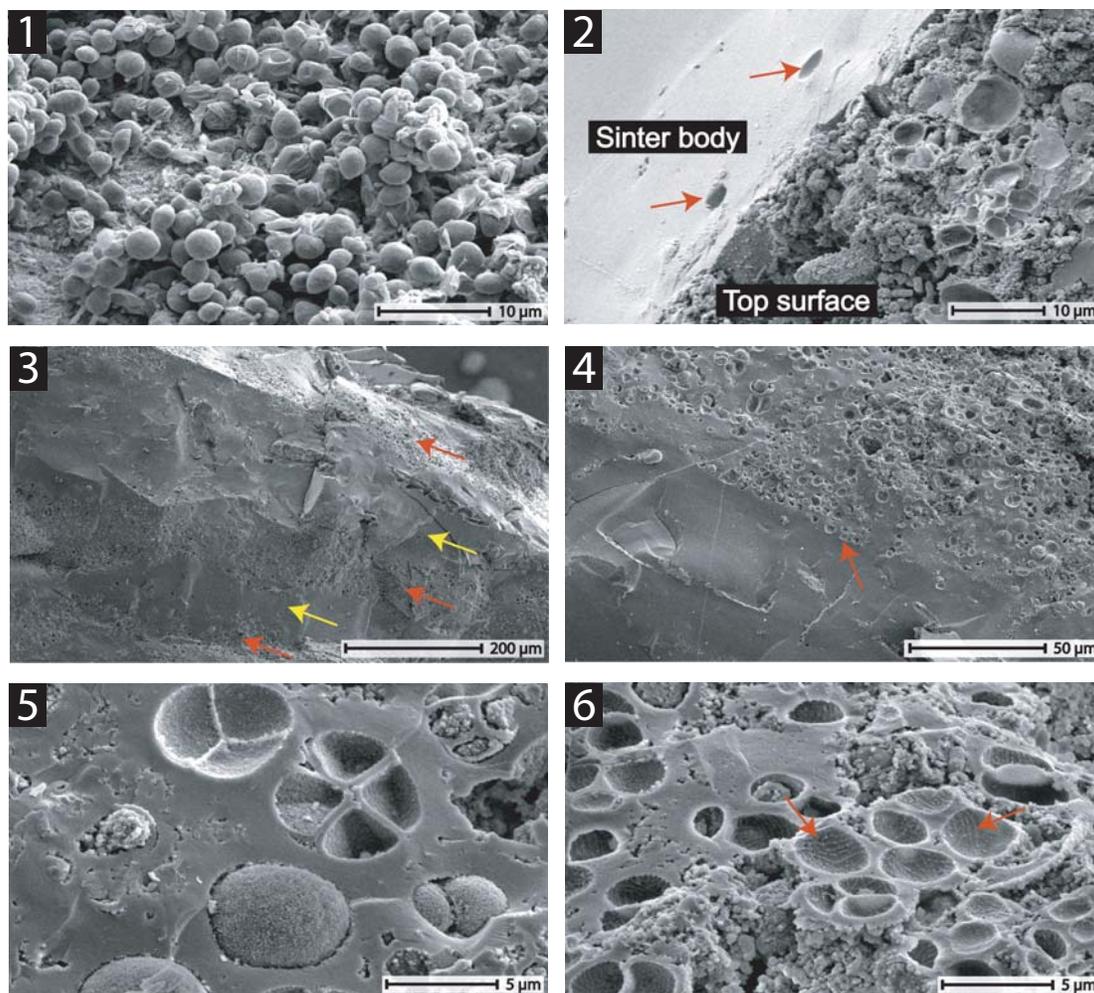
Figure 14. Biotic composition and silicification of green algal-dominated mats on *Microfacies 2* sinter. (1) Overview of an unsilicified green mat showing a predominance of spherical cells that are 2-4 µm in diameter. Minor amounts of bacilli are also present. (2) Silicified portion of a green mat on the top (young) sinter surface. Note the incorporation of equivalent sized spherical cells into the (older) sinter body (red arrows) (cf. Figure 11.6). (3) Alternating laminae of sinter composed of silicified biomats (red arrows) and layers of featureless, massive, vitreous silica (yellow arrows). (4) Sharp boundary (red arrow) between a biotic and an abiotic layer. (5) Close-up of silicified cells incorporated into sinter beneath living green mat. Some silicified cells include endospores. (6) Preservation of cellular impressions (red arrows).

Subaerial Silica Precipitation and the Role of Microorganisms

Abiotic precipitation of silica was shown previously to occur where silica-rich waters wet subaerial substrates, resulting in increased silica oversaturation due to cooling and evaporation (e.g., Weed 1889; Krauskopf 1956; Walter et al. 1972; Rimstidt and Cole 1983; Hinman and Lindstrom 1996; Renaut et al. 1998; Campbell et al. 2002; Mountain et al. 2003). In the Parariki outflows, monomeric silica polymerises and deposits opal-A as the water cools and evaporates (Teece 2000). However, the acid pH at the site slows silica from precipitating subaqueously by inhibiting monomeric silicic acid from deprotonating, polymerising, and nucleating (cf. Iler 1979; Makrides et al. 1980; Weres et al. 1981; Mountain et al. 2003). This inhibition explains both the monomeric form of dissolved silica in the Parariki outflows and the lack of subaqueous silica deposition. The low propensity for silicic acid to polymerise in acid environments is responsible for the small size (<100-500 nm) of the opal-A spheres that comprise the Parariki sinters (cf. Iler 1979). However, monomeric silica may also deposit directly onto the subaerial substratum. Direct monomeric deposition, concomitant with precipitation of small silica spheres, can result in the formation of the massive
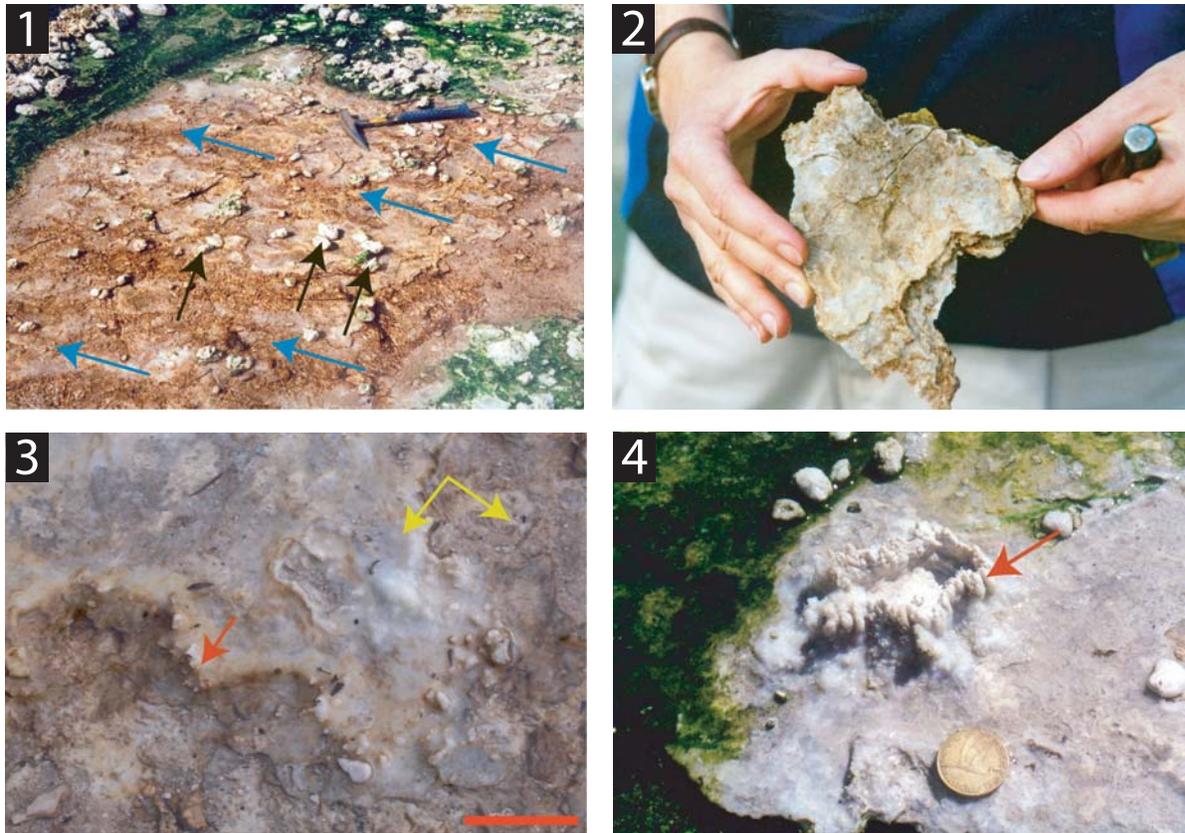
Figure 15. Field occurrences and morphologies of *Microfacies 3* sinter. (1) Flat, sinter deposit (brown colour) over which thermal water flows (blue arrows). *Microfacies 2* sinter forms on pumice clasts above water level (black arrows). Hammer to the upper right is ~30 cm long. (2) Close-up of *Microfacies 3* sinter showing irregular surface texture. (3) Patchy silicification (yellow arrows) and the beginnings of rim formation (red arrow). The rims are frequently above water level. Bar represents 2 cm. (4) Formation of a cup-like deposit (red arrow) that is continuous with the flat, parallel laminated sinter below. Coin is 2.5 cm wide.

vitreous silica texture observed in the cross-sections of all sinters examined in this study (cf. White et al. 1956; Rimstidt and Cole 1983; Handley et al. 2005).

While diatoms take up silicic acid from the water to form their tests, prokaryotes are not known to actively precipitate silica by metabolic activity (Mountain et al. 2003; Konhauser et al. 2004). In this study, it appears that the silicification of microbes and their associated EPS is a passive process. Silicification often does not proceed evenly on the biofilms of Parariki sinters, but is concentrated in places that are more prone to cooling and evaporation, such as the upper portions of microcolonies and spicules (Figure 6) (cf. Jones and Renaut 1997; Lowe and Braunstein 2003). Recent experiments have shown that silica precipitation is affected by its concentration but is independent of microbial growth (Toporski et al. 2002; Yee et al. 2003; Benning et al. 2004). Nevertheless, microbial cell surfaces at the Parariki site

seem to act as favourable nucleation sites for silica precipitation and polymerisation. Silica shows an affinity with functional groups on proteins and polysaccharides of cell walls and EPS (e.g., Schultze-Lam et al. 1995; Westall et al. 1995; Konhauser and Ferris 1996; Renaut et al. 1998; Farmer 1999; Asada and Tazaki 2001; Konhauser et al. 2001). However, microbial silicification in acidic conditions may differ from those in near-neutral to alkaline waters. Acidophilic microbes, for example, may act as reactive interfaces that promote silica nucleation and enhance precipitation kinetics (Fortin and Beveridge 1997). Furthermore, the cell walls of some acidophiles are considered to adsorb hydrogen ions to their surfaces, forming a static barrier against proton (H^+) influx into cell interiors (Gimmler et al. 1989; Asada and Tazaki 2001). Asada and Tazaki (2001) suggested that highly reactive silica ions could be generated in acidic hot springs when adsorbed hydrogen ions combine with monomeric silicic acid, promoting sil-
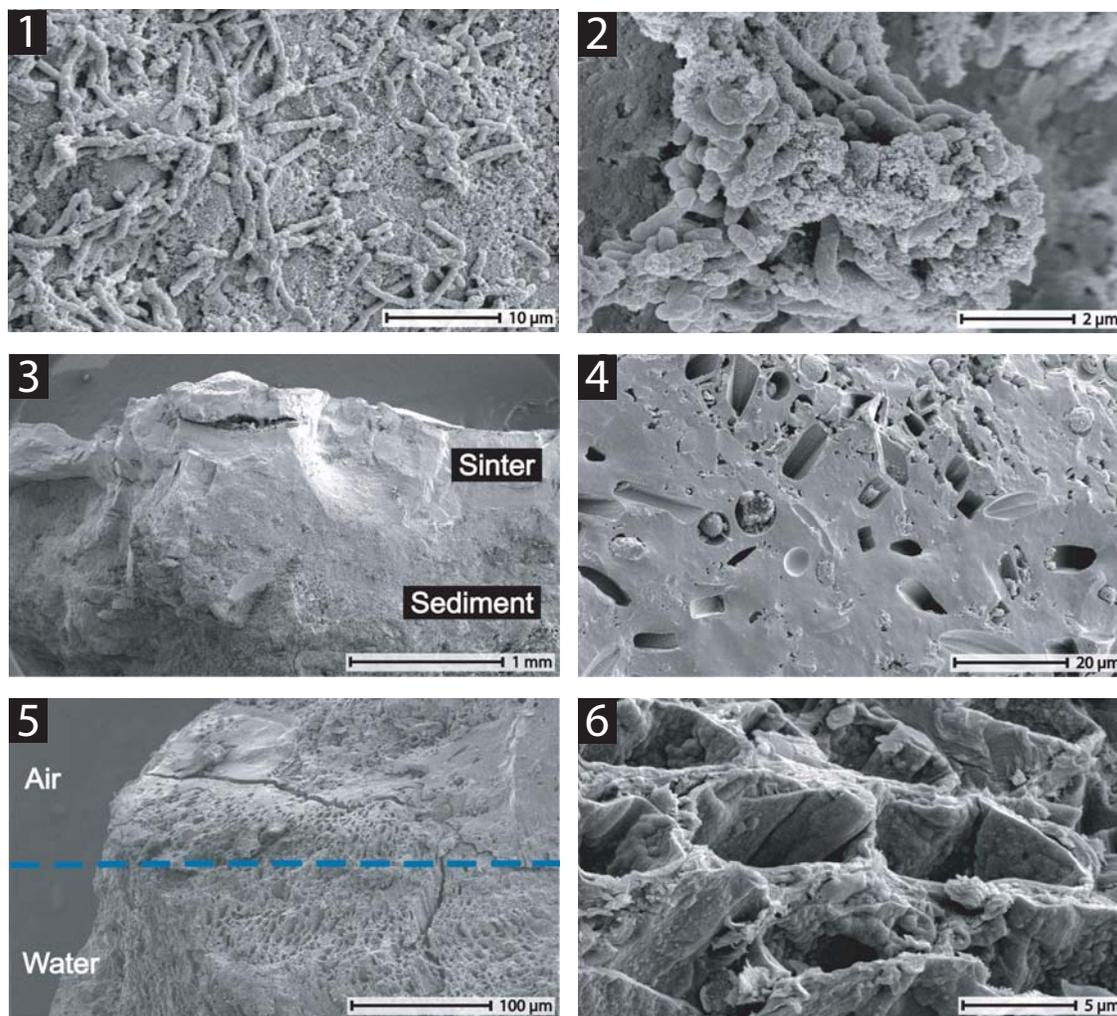
Figure 16. Biotic characteristics and textures of *Microfacies 3* sinter. (1) Colonisation of sinter surface by bacilli. (2) Patchy silicification of cells by nanospheres (<100 nm) of silica. (3) Overview of sinter section showing a predominantly massive, vitreous texture, although cavities are also present. Silicified, sandy sediment underlies sinter. (4) Diatoms and spherical cells cemented into sinter. (5) Clusters of cemented pennate diatoms aligned perpendicular to the approximate air-water interface (dashed blue line). (6) Close-up of (5) showing aligned pennate diatoms.

ica polymerisation if a steady supply of silicic acid is provided.

Microbial silicification at the Parariki site is also important for the textural development of these sinters. Mountain et al. (2003) noted that the small silica sphere sizes occurring in low pH waters can produce a dense silica matrix that accurately preserves microbial matter. In this study, small sphere sizes resulted in the intricate preservation of microbial cell outlines and their EPS (Figures 6, 7 and 12). The precipitation of opal-A spheres on diatom tests and their eventual cementation at the Parariki site shows that these tests can act as sites upon which silica precipitates (cf. Campbell et al. 2004; Jones et al. 2000). Indeed, microbial silicification occurs on all morphotypes at the Parariki site, although species-specific patterns of silicification have been noted elsewhere (e.g., Francis et al. 1978; Westall et al. 1995; Toporski et al. 2002; Lalonde et al. 2005). The tendency of silica to deposit on the margins of diatoms and EPS (Figure 18.2) is likely due to the higher energy encountered at these surfaces (Banfield and Hamers 1997). Atoms on edges have lower coordination and strongly asymmetric bonding configurations (Banfield and Hamers 1997), thereby allowing preferential deposition of silica. The patchy nature of microbial silicification on Parariki sinters (Figure 16.2) may be induced abiotically, or by continuous microbial growth and cell division. The latter would enable microbial populations to survive during constant bathing by silica-rich thermal outflow.
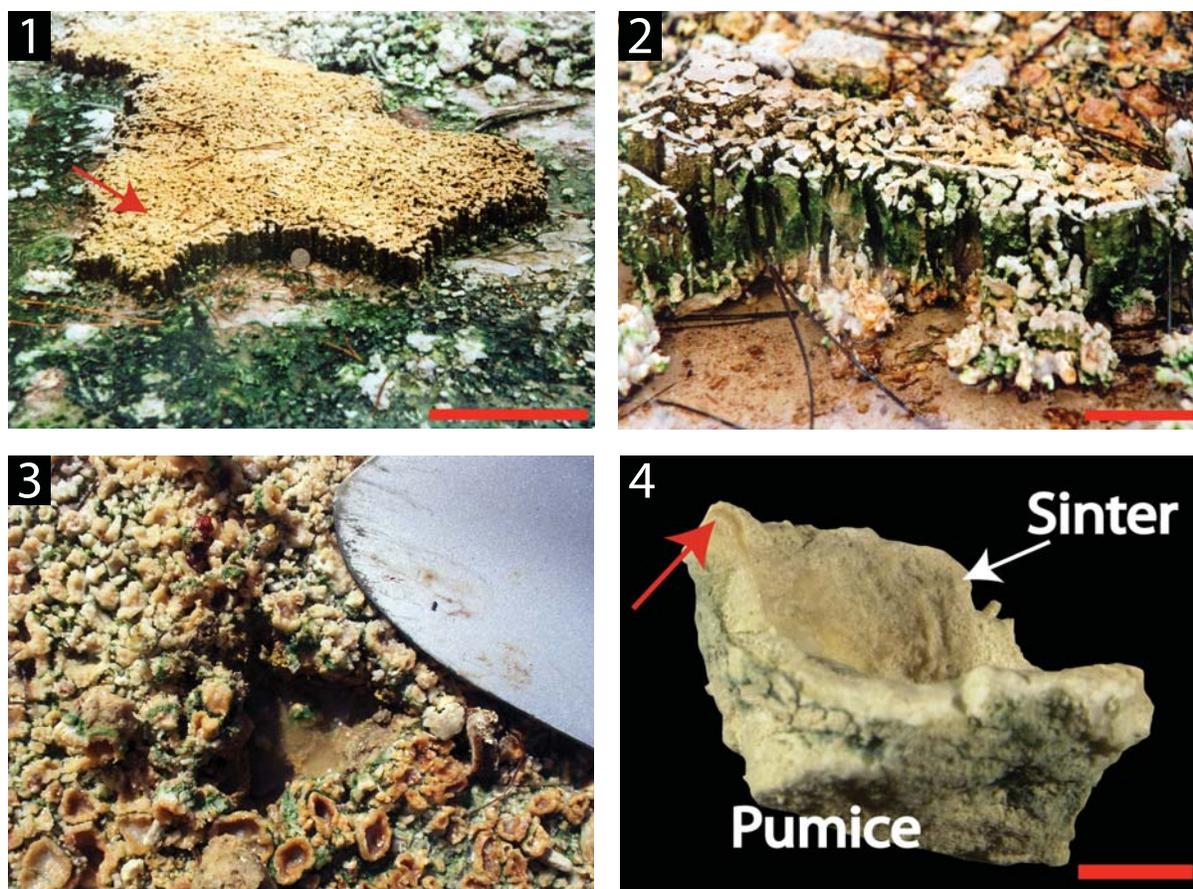
Figure 17. Field occurrences and hand specimens of *Microfacies 4* sinter. (1) Thin siliceous sinter rims (orange colour, red arrow) forming on small pumice clasts that rest on fine sandy substrates. Coin in the centre of photo is 2 cm wide. Bar represents ~15 cm. (2) Close-up showing underlying sandy substrate (covered by green microbial mat) that is protected from erosion by the overlying orange sinter, thereby forming pillar-like structures. Bar represents 4 cm. (3) Small hole dug into the sandy substrate revealing warm (45°C) thermal pore water at shallow depths. Shovel to the upper right is 15 cm wide. (4) Vertical section through a thin siliceous rim sinter. Pumice clast underneath sinter is covered with green microbial mat. Red arrow indicates thin internal laminae that are convex in shape. Bar represents 0.8 cm.

Subaerial Constraints on Sinter Dimensions and Morphogenesis

The formation mechanisms and morphology of Parariki sinters are primarily the products of substrate shape and size and the specific environment. Silica-rich water reaches subaerial substrates in the outflows through water level changes, wave wash and likely through capillary creep. However, these mechanisms are microfacies dependent, and do not occur everywhere at the study site.

In *Microfacies 1-3*, fluctuating water levels enable thermal outflows to reach subaerial portions of various substrates. Subsequent cooling and evaporation ensue, allowing dissolved silica to become oversaturated and deposit as continuous layers. Wave wash, caused by the pulsating dis-charge of thermal water, produces a similar effect. However, this mechanism is largely confined to *Microfacies 1*, where relatively vigorous vent discharge occurs.

Substrate width and shape governs the extent of siliceous covering. On substrates that are relatively wide and higher above water, silica reaches only the margins, producing a ring-like structure. Continuous accumulation of silica between spicules can form a rim (cf. Handley 2004), which, if high enough, blocks further silica deposition inwards. Smaller substrates (e.g., pumice pebbles), in turn, allow silica-rich water to reach surfaces evenly, resulting in sinters that cover the entire original surface. A similar process was suggested to form thrombolites at Lake Clifton, Western Australia (Moore and Burne 1994), and micro-
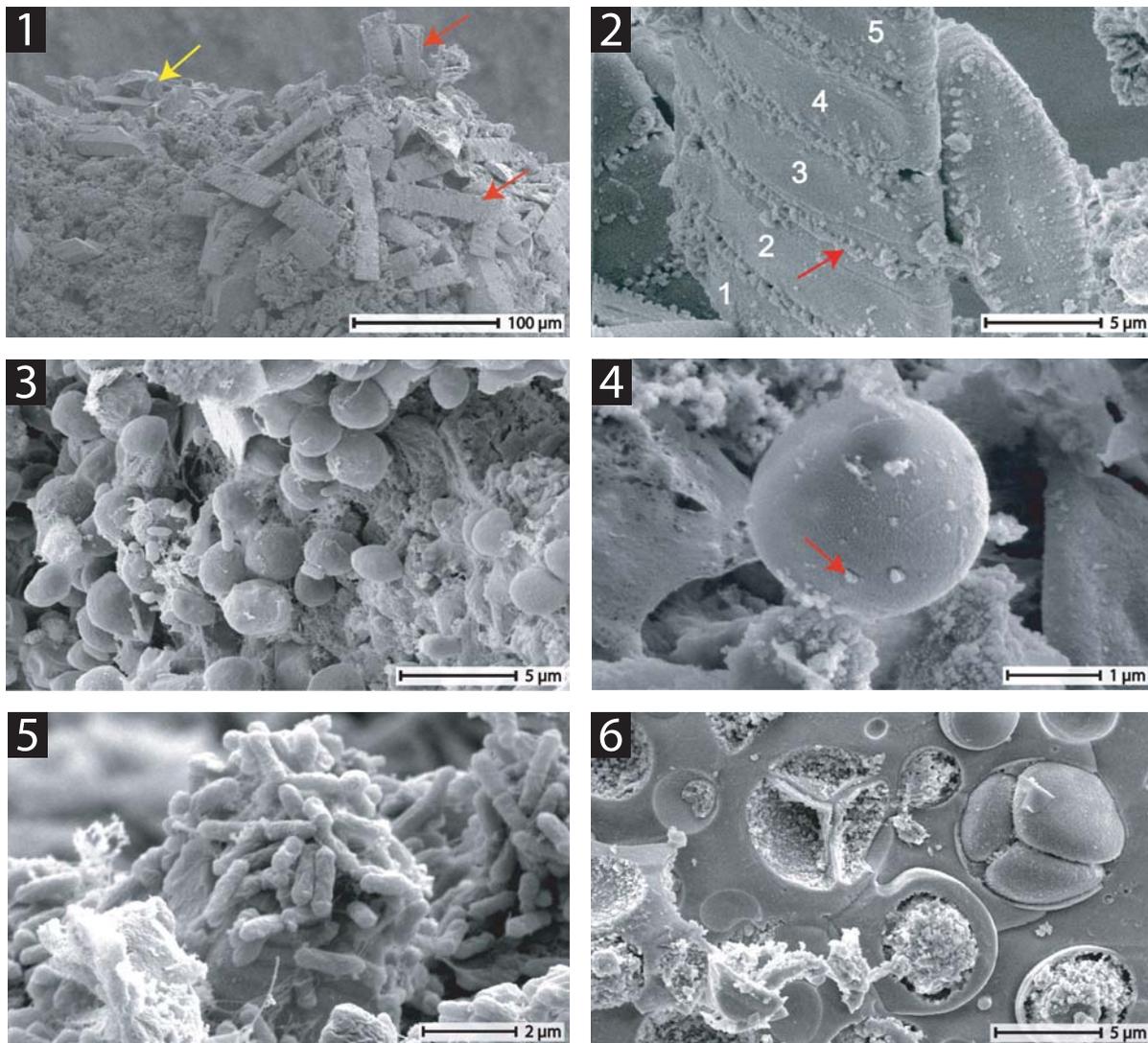
Figure 18. Biotic characteristics and textures of *Microfacies 4* sinter. (1) Clusters of interconnected diatoms (red arrows) distributed on the surface of the sinter rim. Yellow arrow points to gypsum. (2) Close-up of interconnected diatoms (numbered), with silica spheres (~250 nm) precipitating on test margins (red arrow). (3) Colonisation of sinter surface by spherical cells. (4) Spherical cell with silica precipitating on its surface (red arrow). (5) Vertically upright microcolony of bacilli on a diatom test. (6) Incorporation of spherical cells, including endospores, into sinter.

atolls in modern corals (Stoddard and Scoffin 1979). In these two cases, upward growth is constrained by local water level, and subaerial exposure of the upper surfaces restricts growth to the margins (Stoddard and Scoffin 1979; Moore and Burne 1994).

The local energy of the thermal waters surrounding substrates can also affect sinter morphology. In *Microfacies 1*, where relatively more turbulent conditions prevail, silica-rich water reaches greater subaerial portions of the substrates compared to area- and shape-equivalent deposits in *Microfacies 2*. Hence, sinters from the former exhibit a greater extent of siliceous coating than those from *Microfacies 2* and *4*, where more quiescent conditions prevail. In places where thermal water availability is low due to an increasingly sandy substratum, only the margins of substrates become silicified. The resulting deposits are observed in parts of *Microfacies 2* (Figure 10.4) and, especially, *Microfacies 4* (Figure 17), where thermal water moves around increasingly finer grain sizes between adjacent sinter substrate deposits.

Capillary creep and/or diffusion may also play a role in subaerial sinter formation (cf. Henley

1996; Hinman and Lindstrom 1996; Renaut et al. 1998, 1999; Campbell et al. 2002; Guidry and Chafetz 2002; Mountain et al. 2003), particularly for the cup-shaped deposits of *Microfacies 4*. Substrates there are neither exposed to changing water levels, nor are they affected by wave wash. Thermal pore water that is present within the sandy substrate is therefore most likely drawn up towards the surface by capillary rise or diffusion. An upward rise of thermal water would explain the often near-vertical rims of these deposits and their confinement to only the small pumice substrate margins. In this scenario, the margins form convex-upward laminae (Figure 17.4). Small, calcareous stromatolitic structures of similarly low relief (<5 cm in diameter) occur on a sandy shoreline at Lake Clifton, Western Australia (Moore and Burne 1994). Even when exposed by low lake levels during summer, these stromatolites remain saturated by low salinity groundwater seepage through capillary action (Moore and Burne 1994).

In *Microfacies 3*, silica precipitation will be slowed by the acidic discharge that flows over the flat, parallel-laminated deposits (Figure 15.1). However, periodic exposure above the water and concomitant cooling and evaporation of remaining puddles of silica-rich water would allow for sinter to accumulate. The patchy silicification of these sinters (Figure 15.3) is likely a result of cooling and evaporation of local puddles of thermal water. However, other factors not identified in this study may also play a role in the formation of *Microfacies 3* sinter.

Significance of Microbial Biofilms upon Sinter

Biofilms can afford protection from environmental extremes (Hall-Stoodley et al. 2004), which are common in an acid hot spring setting: low pH (McNeill and Hamilton 2003); metal toxicity (Teitzel and Parsek 2003); dehydration and high salinity (Le Magrex-Debar et al. 2000; Sutherland 2001); and UV exposure (Espeland and Wetzel 2001). In addition, associated EPS may prevent cell silicification by providing reactive sites for silica to bind (Lalonde et al. 2005). According to contemporary models (e.g., Stoodley et al. 2002), the formation and development of prokaryotic biofilms requires the transport of microbes to a surface and their initial attachment, followed by microcolony formation. In quiescent waters of low-shear, laminar flow, and with ideal nutrient conditions, microcolonies often resemble pillar, mushroom, or mound-like structures (e.g., Hall-Stoodley and Stoodley 2002; Stoodley et al. 2002; Hall-Stoodley et al. 2004;

Purevdorj et al. 2002). These morphologies are formed by clonal division, whereby daughter cells spread outwards and upwards from the attachment surface to form cell clusters (Hall-Stoodley and Stoodley 2002; Stoodley et al. 2002). Microcolonies on the Parariki sinters also exhibit positive relief, with both bacilliform and coccoidal prokaryotic microorganisms developing vertically upright structures. At the Parariki site, lobed coccoidal and bacilli morphotypes also were confined to different microfacies settings, with the former largely restricted to *Microfacies 1*, and the latter observed elsewhere at the site. Similar differential distributions of microbial morphotypes occur in acid hot springs at Yellowstone (e.g., Brock 1978), Italy (Simmons and Norris 2002), and Montserrat (Burton and Norris 2000). In these studies, lobed coccoidal prokaryotic microorganisms (e.g., *Sulfolobus*) occur in higher temperature settings (usually >60°C), while bacilli (e.g., *Thiobacillus*) are found in the relatively cooler waters (>30°C).

Apart from prokaryotes, algae, particularly diatoms and members of the Cyanidiophyceae, are ubiquitous in the relatively cooler waters (52.5°C) at the Parariki site. The predominance of algal mats at the study site is consistent with previous studies of acidic hot springs in New Zealand (Brock and Brock 1971; Brock 1978; Cassie and Cooper 1989; Jones et al. 2000) and elsewhere (e.g., Brock 1973, 1978; Gross 1998; Seckbach 1998; Ferris et al. 2005; Walker et al. 2005). The role of Cyanidiophyceae-dominated biofilms in the formation of laminae is discussed below. Diatom biofilms also are an important constituent of sinters from *Microfacies 2-4*, where waters are cool enough for diatom survival (typically 45°C; Cassie 1989). Benthic diatoms that are adnate, or closely appressed to the substratum, like those at the Parariki site, tend to be motile (Cohn and Dispari 1994; Cohn and Weitzell 1996). Such diatoms glide up through sediments in a movement that is non-random, following distinctive sets of chemotactic and phototactic responses (Cohn and Disparti 1994; Cohn and Weitzell 1996). EPS secretion by these organisms is also used for their daily migrations across surfaces (Cohn and Weitzell 1996).

Diatoms that attach to siliceous deposits at the Parariki site prefer to inhabit areas of low microrelief, such as pits, cracks, and along small cavities (Figure 13.1-13.3). In studies conducted elsewhere, protective areas were shown to provide refugia for diatoms from grazers (e.g., Dudley and D'Antonio 1991), shield them from abrasion and drag associated with moving water (Luttenton and

Rada 1986), and protect them from desiccation (Hostetter and Hoshaw 1970). The effects of grazing activity on diatoms at the Parariki site are unknown. However, the presence of numerous clumps of fractured diatom shells indicates that water is turbulent enough in places to crush diatom tests and transport them (Figure 13.5). Repeated wetting and drying of the siliceous deposits could also cause significant stress to diatoms.

While a preponderance of diatoms has been noted in other acid hot spring settings (Jones et al. 2000), no fungi were observed on Parariki sinters. This observation is in contrast to previous studies of acid hot spring deposits, where fungi are purported to be dominant (Jones et al. 1999, 2000).

Origins of Spiculose Textures

While spicules from the Parariki sinters are similar in their gross morphology to spicular geyserite around spouters (cf. Walter 1976; Braunstein and Lowe 2001; Jones and Renaut 2003; Lowe and Braunstein 2003), there are also distinctive differences between them. Spicular geyserite forms at the air-water interface where water splashes around the inner rims of springs (Walter 1976). While biofilms are present on spicular geyserite and help form porous laminae (Cady and Farmer 1996), the formation of these spicules is largely attributed to abiotic mechanisms, involving splash and spray of silica-rich waters (Walter 1976; Braunstein and Lowe 2001; Jones and Renaut 2003; Lowe and Braunstein 2003). Spicules that form this way tend to be larger at the poolward sides of rims, where greater wave activity and splash occurs, than on the landward sides (Walter 1976; Lowe and Braunstein 2003). At the Parariki site, by contrast, neither splash nor spray was observed, and spicules are progressively larger *away* from the water. Furthermore, the Parariki spicules are bigger where water is more quiescent, with longer spicules in *Microfacies 2* (1 cm in high), than in the more turbulent *Microfacies 1* (0.5 cm high) environment. In the latter, spicules occur only on the uppermost portions of the sinters, away from the thermal waters, and within cavities (Figure 5.2). Thus, the spiculose Parariki sinter textures must develop by mechanisms different from those of classic spicular geyserite.

In previous studies, biotic mechanisms for spicular sinter formation have also been proposed (Cassie and Cooper 1989; Campbell et al. 2002) and shown to be facilitated by filamentous microbes at Champagne Pool, New Zealand (Handley et al. 2005). In this study, microspicule initia-

tion and development was observed to involve a dynamic interplay between biofilm growth and silica deposition. Vertically upright colonies of micro-organisms (coccoidal and bacilliform) were observed to act as domains of positive relief that commonly became progressively silicified and subsequently recolonised (cf. Handley et al. 2005). The restriction of these microspicules to quiescent sinter portions correlates with the distribution of their macroscopic counterparts.

It was beyond the scope of this study to establish causes governing the development of the Parariki biofilm morphologies. However, biofilm development is a multifactorial process influenced by both environmental factors and genes (Hall-Stoodley et al. 2004). Previous studies have shown how environmental conditions, such as water flow, including turbulence, can potentially affect biofilm development, superseding cell-cell communications as a principal determinant of biofilm morphogenesis (Hall-Stoodley and Stoodley 2002; Purevdorj et al. 2002). The tendency for vertically upright microcolonies to form in less turbulent waters may therefore explain the restriction of the Parariki spicules to more quiescent areas. Nevertheless, environmental factors other than water turbulence, such as nutrient availability and phototrophy, may also play a role (e.g., Doemel and Brock 1974; Brock 1978; Stoodley et al. 2002; Hall-Stoodley et al. 2004). However, for spicule formation to proceed and continue, the supply of silica is likewise important. In *Microfacies 4*, thermal water is confined to pore spaces within the sandy substrate. Water is not turbulent there and sinters experience only minor contact with thermal water. Therefore, sinter growth rates are slowest in that setting and spicules are generally absent, although vertically upright microcolonies are present. Hence, balances between environmentally induced biofilm morphogenesis and the supply of silica-rich water are most likely the major determinants of spicule formation and growth at the Parariki site (cf. Handley et al. 2005). Fluctuations in the supply of silica would reinforce or dampen spicule growth by the deposition of successive silica laminae (Figure 11.3). Such fluctuations could be achieved by dilution of the thermal water by rain water or diurnal or seasonal variations in temperature.

The occurrence and preservation of spicular textures in fossil sinter deposits may be of importance to palaeoenvironmental analysis. However, care should be applied when interpreting textures. As noted above, spiculose sinters can occur in both quiescent and in turbulent conditions, the lat-

ter producing geyserite. Therefore, spiculose textures in ancient hot spring deposits should not be taken as the sole facies indicator of water turbulence but considered in context with other proxies (e.g., oncoids and pisoids; silicified streamers; preserved sinter terraces) (e.g., Walter et al. 1996; Campbell et al. 2001).

Morphogenesis of Ridges, Cavities, Nodules, and Isolated Remnants

Anastomosing ridges, associated cavities, nodules, and pits that occur on surfaces of *Microfacies 1* sinter were seen previously on siliceous sinter (Braunstein and Lowe 2001; Lowe and Braunstein 2003) and silica residue (Cook et al. 2000; Rodgers et al. 2002, 2004). For sinter, constructive processes were inferred for their formation. Such constructive processes result when pits retain water between wetting events from geyser eruptions, while capillary action and evaporation draw water along edges, forming rims alongside these pits through concomitant deposition of silica (Lowe and Braunstein 2003, figure 20A). In cross-section, these deposits are typically composed of cavities and pseudo-cross-laminae that mark pit migration (Lowe and Braunstein 2003, figure 20B, C). Micropitted nodular sinters, or "knobs," are also suggested to form from repeated wetting and drying (Braunstein and Lowe 2001, figure 12B).

The formation of ridges, cavities, and nodules on *Microfacies 1* sinter at the Parariki site may involve a similar component of construction. However, destructive processes in acid settings should not be discounted. Ridge formation does not necessarily require repeated wetting events by silica-rich water, as similar irregular ridges have been observed to form in sinter buried in humate-rich soil that was exposed to rain water (B.Y. Lynne, personal commun., 2004). Nodules, similar in shape to those in the Parariki sinters of *Microfacies 1*, also occur on siliceous coverings of pumice on steaming ground at Rotokawa (R. Schinteie, unpublished data).

Anastomosing ridges on silica residue are interpreted to be destructive remnants of surfaces etched by dissolution (Cook et al. 2000; Rodgers et al. 2002, 2004). Alongside these ridges, layers of once-cemented opal-A microspheres become exposed, while depressions between the ridges are lined by irregular clusters of silica spheres at different stages of dissolution (cf. Rodgers et al. 2002, figure 8). Corrosive activity could likewise produce the gnarly texture (Figure 5.4), necking (Figures 8.6, 9.2 and 9.6), and the dominance of

larger ridges on the outermost sides of isolated remnants (Figure 9.4 and 9.6) on *Microfacies 1* sinter. Corrosive attack focused around edges, kink sites, or necks would likely occur due to the lower coordination number and hence lower energy encountered in these locations (cf. Banfield and Hamers 1997).

Cross-sections of Parariki sinters, seen in thin section and under SEM, reveal that they are massive in texture, with neither open cavities nor pseudo-cross-laminae present. Therefore, the ridge and cavity morphology is only a surface feature. A later-stage deposition of silica would bury these irregular surface textures.

Steam condensate, made acid by the oxidation of H_2S, is often cited as the cause of corrosion of silica residue or sinter surfaces close to vents or steaming ground (e.g., Rodgers et al. 2002; Jones and Renaut 2003; Lynne and Campbell 2004). Complexing of silica by sulphate has been suggested to increase amorphous silica solubilities in aqueous Na_2SO_4 solutions (Marshall and Chen 1982; Fournier and Marshall 1983). Acid steam condensate may therefore explain the restriction of corrosive-like textures to predominantly *Microfacies 1* sinter where copious steam emission occurs. However, further research is warranted.

Changes in Silica Sphere Morphology

The ill-defined silica-spheres (Figure 8.1-8.2) in *Microfacies 1* sinter superficially appear as if they were covered by microbially induced, mucus-like substances. However, the pervasive nature of this texture and the lack of association with microorganisms may call for alternative explanations. Similarly ill-defined sphere shapes have been observed on acid-formed sinters elsewhere and attributed to repeated episodes of silica dissolution and redeposition, causing a blurring of particle detail (Rodgers et al. 2004). Silica solubility is greater on convex surfaces than on concave surfaces (Iler 1979). Hence, silica spheres become obscure in form as silica dissolves from the upper convex surfaces and redeposits on the concave surfaces, where solubility is lower. This process forms "interparticle necks." Rodgers et al. (2004) suggested that changes in microchemical conditions were responsible for the episodic nature of silica dissolution and redeposition in acid water derived sinters. Similarly, near fumaroles, indistinct opal-A spheres form closely packed aggregates (Lynne and Campbell 2004). In silica residue, gelatinous, ill-defined spheres (also referred to as "frog spawn" texture) form and are purported to be

the result of progressive strengthening of interparticle bonds at the contact between adjacent silica spheres (Rodgers et al. 2002, 2004).

Origins of Sinter Laminae

While laminae in Parariki sinters of all microfacies were visible in hand sample and/or in thin section, they were not observed under SEM, where vertical sections mostly revealed a massive, vitreous sinter body (e.g., Figure 16.3). However, the irregular, gnarled surfaces on *Microfacies 1* sinter exhibited layering under SEM (Figure 9.5), while for *Microfacies 2* deposits, a succession of silica layers was observed only at the surface (Figure 13.3). Jones and Renault (2004) related indistinctive laminae in other sinters to differences in the water contents of opal-A. Since these differences are texturally featureless, they are not detected by standard SEM methods. However, etching of these surfaces, attributed to acidic steam condensate, reveals alternating laminae caused by differential dissolution of opal-A due to local differences in silica solubility (Jones and Renaut 2003, 2004). Jones and Renaut (2004) interpreted "wet" opal layers to be formed by rapid precipitation of hydrated silica. "Dry" opal, in turn, would form by slow evaporation, resulting in layers of silica with less water. Since the Parariki sinters also form by repeated wetting and drying, a continuous laminated buildup would likewise develop.

Lower portions of sinter from *Microfacies 2*, by contrast, consist of laminae that are both abiotic and biotic in nature. Green, algal-dominated mats cover a large portion of these sinters close to the air-water interface (Figure 10), and become silicified and incorporated into the sinter (Figure 14). Studies of the taxonomically related alga *Cyanidium caldarium*, suggest that silicification of its mats result by the continuous proliferation of non-motile algal cells, with parental cells underlying younger cells (Asada and Tazaki 1999). Therefore, older cells will face shortages of light and CO_2 for photosynthesis, and O_2 for respiration. Asada and Tazaki (1999) suggested that these stresses impair the ability of the algal cells to regulate silica on their walls, so that silica continuously grows on them and progressively fills the interstices between silica crusts of different cells.

The restriction of the green Parariki algal mats to the lower portions of *Microfacies 2* sinters (Figures 10 and 11.5) could be temperature controlled, although moisture and nutrient supply may also influence their distributions. Brock (1978) found *C. caldarium* cells growing in high densities at ~45°C throughout its range (55-20°C). Indeed, the green mats from our study are thickest (1 mm) close to the water level at *Microfacies 2* (50-40°C), and gradually disappear closer to the upper portions of the sinters. On the higher substrate areas of *Microfacies 2* sinters, where green mats are absent, silica layering occurs only as fine laminae in thin-section and as a succession of silica horizons under SEM (Figure 13.3, red arrows), with no apparent microbial association. Continuous deposition of silica by wetting and drying appears to be the principal method of forming these abiotic laminae in the upper areas.

Stromatolitic Nature of Parariki Sinters

The sinters forming at the Parariki study site are laminated growth structures, morphologically similar in appearance to stromatolites described around other hot springs. However, the criteria used to define stromatolites are not straightforward because the search for a clear and widely accepted definition of them has proven controversial (Ginsburg 1991; Cady et al. 2003). Generally, most authors define stromatolites as layered organosedimentary structures, formed by the trapping, binding, and/or precipitation of sediments as a result of the growth and metabolic activity of microorganisms (Walter 1976; Krumbein 1983). However, the lack of fossilised microbes in many ancient stromatolites, or the potential for stromatolitic laminae to be formed entirely by abiotic means (Grotzinger and Rothman 1996) has caused problems with this genetic definition.

At the Parariki site, sinter laminae and textures such as spicules formed as a result of a combination of abiotic and biotic factors. However, taphonomic constraints can affect the differential preservation of microorganisms. At the Parariki site, ubiquitous microbial mats of prokaryote-sized microorganisms cover sinters from all microfacies. Nevertheless, preservation of these microbes as distinct, silicified laminae is often absent or confined to spicules. By contrast, algal cells, including diatoms, are much better preserved in Parariki sinter laminae. This differential preservation would bias the potential fossil record in assuming that these sinters were once largely colonised by eukaryotes. Therefore, a descriptive and non-genetic definition of stromatolites has been adopted herein, whereby a stromatolite is described as "an attached, laminated, lithified sedimentary growth structure, accretionary away from a point of limited surface of initiation" (Semikhatov et al., 1979).

CONCLUSIONS

Environmental variables, acting on a micro-scale over a few centimetres (or less) at the Parariki study site, have a differential effect on sinter textures and microbiology. Hence, four different microfacies of stromatolitic sinter occur, featuring distinctive deposit morphologies, textures, formation mechanisms, and microbial communities. Constraints on their distribution include: 1) the size and shape of the subaerial substrate surfaces; 2) the relative exposure to thermal waters; 3) water flow rate; 4) the presence, nature, and taphonomy of mat-forming microorganisms; 5) water and ambient temperature; and 6) potential exposure to acid steam condensate. The dynamic interplay between silica deposition and microbial activity is a major factor in the formation of a variety of sinter textures, particularly spicules. Laminae develop in these sinters due to abiotic and/or alternating abiotic and biotic processes. Different microbial communities also exhibit variable preservation potential as sinter accumulates, regardless of microbial abundances.

Results of this study are consistent with previous studies of acid hot spring deposits. In terms of the associated biota, eukaryotes, namely diatoms and the rhodophyte taxon Cyanidiophyceae, are a ubiquitous sinter component at temperatures <52.5°C. Lobed coccoidal and bacilliform morphotypes of prokaryotic dimensions also were confined to different microfacies settings, with the former largely restricted to the hotter setting of *Microfacies 1*, and the latter observed elsewhere at the site. Clay minerals, as well as fungi, were not observed in this study. Mineralogically, sinters of *Microfacies 1* are similar to silica residue and siliceous deposits around fumaroles; namely a gnarled, possibly corrosive, surface texture and/or faint silica sphere shapes.

ACKNOWLEDGEMENTS

REFERENCES

Asada, R. and Tazaki, K. 1999. Biomineralization of silica under strong acidic conditions. *Proceedings of the International Symposium, Kanazawa, Earth-Water-Humans*, 209-216.

Asada, R. and Tazaki, K. 2001. Silica biomineralization of unicellular microbes under strongly acidic conditions. *The Canadian Mineralogist*, 39:1-16.

Banfield, J.F. and Hamers, R.J. 1997. Processes at minerals and surfaces with relevance to microorganisms and prebiotic synthesis, p. 81-117. In Banfield, J.F., and Nealson, K.H. (eds.), *Geomicrobiology: interactions between Microbes and Minerals.* Mineralogical Society of America, Washington D.C.

Barns, S.M., Delwiche, C.F.D., Palmer, J.D., Dawson, S.C., Hershberger, K.L., and Pace, N.R. 1996. Phylogenetic perspective on microbial life in hydrothermal ecosystems, past and present, p. 24-39. In Bock, G.R., and Goode, J.A. (eds.), *Evolution of Hydrothermal Ecosystems on Earth (and Mars?), Ciba Foundation Symposium 202*. John Wiley and Sons, Chichester.

Benison, K.C. and Laclair, D.A. 2002. Acid sedimentary environments on Mars?: possible terrestrial analogs. *The Geological Society of America, Denver Annual Meeting*, 34:174.

Benning, L.G., Phoenix, V.R., Yee, N., and Konhauser, K.O. 2004. The dynamics of cyanobacterial silicification: an infrared micro-spectroscopic investigation. *Geochimica et Cosmochimica Acta*, 68:743-757.

Bibby, H.M., Caldwell, T.G., Davey, F.J., and Webb, T.H. 1995. Geophysical evidence on the structure of the Taupo Volcanic Zone and its hydrothermal circulation. *Journal of Volcanology and Geothermal Research*, 68:29-58.

Blank, C.E., Cady, S.L., and Pace, N.R. 2002. Microbial composition of near-boiling silica-depositing thermal springs throughout Yellowstone National Park. *Applied and Environmental Microbiology*, 68:5123-5135.

Braunstein, D. and Lowe, D.R. 2001. Relationship between spring and geyser activity and the deposition and morphology of high temperature (>73°C) siliceous sinter, Yellowstone National Park, Wyoming, U.S.A. *Journal of Sedimentary Research*, 71:747-763.

Brock, T.D. 1973. Lower pH limit for the existence of blue-green algae: evolutionary and ecological implications. *Science*, 179:480-483.

Brock, T.D. 1978. *Thermophilic Microorganisms and Life at High Temperatures.* Springer Verlag, New York.

Brock, T.D. and Brock, M.L. 1971. Microbiological studies of thermal habitats of the central volcanic region, North Island, New Zealand. *New Zealand Journal of Marine and Freshwater Research*, 5:233-258.

Browne, P.R.L. 1974. Rotokaua geothermal field. *Minerals of New Zealand, New Zealand Geological Survey, Report No. 38.*

Bullock, M.A. 2005. The flow and ebb of water. *Nature*, 438:1087-1088.

Burton, N.P. and Norris, P.R. 2000. Microbiology of acidic, geothermal springs of Montserrat: environmental rDNA analysis. *Extremophiles*, 4:315-320.

Cady, S.L. and Farmer, J.D. 1996. Fossilization processes in siliceous thermal springs: trends in preservation along thermal gradients, p. 150-173. In Bock, G.R. and Goode, J.A. (eds.), *Evolution of Hydrothermal Ecosystems on Earth (and Mars?), Ciba Foundation Symposium 202*. John Wiley and Sons, Chichester.

Cady, S.L., Farmer, J.D., Grotzinger, J.P., Schopf, W.J., and Steele, A. 2003. Morphological biosignatures and the search for life on Mars. *Astrobiology*, 3:351-368.

Campbell, K.A., Buddle, T.F., and Browne, P.R.L. 2004. Late Pleistocene siliceous sinter associated with fluvial, lacustrine, volcaniclastic and landslide deposits at Tahunaatara, Taupo Volcanic Zone, New Zealand. *Transactions of the Royal Society of Edinburgh: Earth Sciences*, 94:485-501.

Campbell, K.A., Rodgers, K.A., Brotheridge, J.M.A., and Browne, P.R.L. 2002. An unusual modern silica-carbonate sinter from Pavlova spring, Ngatamariki, New Zealand. *Sedimentology*, 49:835-854.

Campbell, K.A., Sannazzaro, K., Rodgers, K.A., Herdianita, N.R., and Browne, P.R.L. 2001. Sedimentary facies and mineralogy of the late Pleistocene Umukuri silica sinter, Taupo Volcanic Zone, New Zealand. *Journal of Sedimentary Research*, 71:727-746.

Cassie, V. 1989. *A contribution to the study of New Zealand diatoms*. Bibliotheca Phycologica, Band 17, J. Cramer, Berlin, Stuttgart.

Cassie, V. and Cooper, R.C. 1989. *Algae of New Zealand thermal areas*. Bibliotheca Phycologica, Band 78, J. Cramer, Berlin, Stuttgart.

Chen, Z.-W., Jiang, C.-Y., She, Q., Liu, S.-J., and Zhou, P.-J. 2005. Key role of cysteine residues in catalysis and subcellular localization of sulfur oxygenase-reductase of *Acidianus tengchongensis*. *Applied and Environmental Microbiology*, 71:621-628.

Cohn, S.A. and Disparti, N.C. 1994. Environmental factors influencing diatom cell motility. *Journal of Phycology*, 30:818-828.

Cohn, S.A. and Weitzell, Jr., R.E. 1996. Ecological considerations of diatom cell motility. I. Characterization of motility and adhesion in four diatom species. *Journal of Phycology*, 32:928-939.

Collar, R.J. and Browne, P.R.L. 1985. Hydrothermal eruptions in the Rotokawa Geothermal System, Taupo Volcanic Zone, New Zealand. *Proceedings of the 7th Geothermal Workshop*, Geothermal Institute, University of Auckland, Auckland, 171-176.

Cook, K.L., Rodgers K.A., Campbell K.A., Browne, P.R.L., Martin, R., and Seakins, J.M. 2000. The mineralogy, texture and significance of silica residue from the Te Kopia geothermal field, Taupo Volcanic Zone. *Proceedings of the 22nd New Zealand Geothermal Workshop*, Geothermal Institute, University of Auckland, Auckland, 143-149.

Doemel, W.N. and Brock, T.D. 1974. Bacterial stromatolites: origin of laminations. *Science*, 184:1083-1085.

Dove, P.M. and Rimstidt, J.D. 1994. Silica-water interactions, p. 259-308. In Heaney, P.J., Prewitt, C.T., and Gibbs, G.V. (eds), *Silica: Physical Behavior, Geochemistry and Materials Applications*. Mineralogical Society of America, Washington, D.C.

Dudley, T.L. and D'Antonio, C.M. 1991. The effects of substrate texture, grazing, and disturbance on macroalgal establishment in streams. *Ecology*, 72:297-309.

Ellis, A.J. and Wilson, S.H. 1961. Hot spring areas with acid-sulphate-chloride waters. *Nature*, 191:696-697.

Espeland, E.M. and Wetzel, R.G. 2001. Complexation, stabilization, and UV photolysis of extracellular and surface-bound glucosidase and alkaline phosphotase: implications for biofilm microbiota. *Microbial Ecology*, 42:572-585.

Farmer, J.D. 1996. Hydrothermal systems on Mars: an assessment of present evidence, p. 273-299. In Bock, G.R. and Goode, J.A. (eds.), *Evolution of Hydrothermal Ecosystems on Earth (and Mars?), Ciba Foundation Symposium 202*. John Wiley and Sons, Chichester.

Farmer, J.D. 1999. Taphonomic modes in microbial fossilization. *Size Limits of Very Small Microorganisms: Proceedings of a Workshop*. Washington National Academy Press, Washington, D.C.

Farmer, J.D. 2000. Hydrothermal systems: doorways to early biosphere evolution. *GSA Today*, 10:2-9.

Farmer, J.D. and Des Marais, D.J. 1999. Exploring for a record of ancient Martian life. *Journal of Geophysical Research*, 104:26977-26995.

Ferris, M.J., Sheehan, K.B., Kühl, M., Cooksey, K., Wigglesworth-Cooksey, B., Harvey R., and Henson, J.M. 2005. Algal species and light microenvironment in a low pH, geothermal microbial mat community. *Applied and Environmental Microbiology*, 71:7164-7171.

Foged, N. 1979. *Diatoms in New Zealand, the North Island*. Bibliotheca Phycologica, Band 47, J. Cramer, Berlin, Stuttgart.

Forsyth, D.J. 1977. Limnology of Lake Rotokawa and its outlet stream. *New Zealand Journal of Marine and Freshwater Research*, 11:525-539.

Fortin, D. and Beveridge, T.J. 1997. Role of the bacterium *Thiobacillus* in the formation of silicates in acidic mine tailings. *Chemical Geology*, 141:235-250.

Fournier, R.O. 1985. The behavior of silica in hydrothermal solutions, p. 45-61. In Berger, B.R. and Bethke, P.M. (eds.), *Geology and Geochemistry of Epithermal Systems*, Society of Economic Geologists.

Fournier, R.O. and Marshall, W.L. 1983. Calculation of amorphous silica solubilities at 25° to 300°C and apparent cation hydration numbers in aqueous salt solutions using the concept of effective density of water. *Geochimica et Cosmochimica Acta*, 47:587-596.

Francis, S., Margulis, L., and Barghoorn, E.S. 1978. On the experimental silicification of microorganisms II. On the time of appearance of eukaryotic organisms in the fossil record. *Precambrian Research*, 6:65-100.

Gimmler, H., Weiss, U., and Weiss, C. 1989. pH-regulation and membrane potential of the extremely acid resistant green alga *Dunaliella acidophila*, p. 389-390. In Dainty, J. (ed.), *Plant Membrane Transport*. Elsevier Science, Venice.

Ginsburg, R.N. 1991. Controversies about stromatolites: vices and virtues, p. 25-36. In Müller, D.W., McKenzie, J.A., and Weissert, H. (eds.), *Controversies in Modern Geology*. Academic Press Limited, London.

Grange, L.I. 1937. *The geology of the Rotorua-Taupo subdivision*. Department of Scientific and Industrial Research, Geological Survey Bulletin No. 37, Wellington.

Gross, W. 1998. Revision of comparative traits for the acido- and thermophilic red algae *Cyanidium* and *Galdiera*, p. 439-447. In Seckbach, J. (ed.), *Enigmatic microorganisms and life in extreme environments*. Kluwer Academic Publishers, Boston.

Grotzinger, J.P. and Rothman, D.H. 1996. An abiotic model for stromatolite morphogenesis. *Nature*, 383:423-425.

Guidry, S.A. and Chafetz, H.S. 2002. Factors governing subaqueous siliceous sinter precipitation in hot springs: examples from Yellowstone National Park, USA. *Sedimentology*, 49:1253-1267.

Guidry, S.A. and Chafetz, H.S. 2003. Anatomy of siliceous hot spring: examples from Yellowstone National Park, Wyoming, USA. *Sedimentary Geology*, 157:71-106.

Hall-Stoodley, L. and Stoodley, P. 2002. Developmental regulation of microbial biofilms. *Current Opinion in Biotechnology*, 13:228-233.

Hall-Stoodley, L., Costerton, J.W., and Stoodley, P. 2004. Bacterial biofilms: from the natural environment to infectious diseases. *Nature Reviews Microbiology*, 2:95-108.

Handley, K.M. 2004. In situ *experiments on the growth and textural development of subaerial microstromatolites, Champagne Pool, Waiotapu, NZ*. Unpublished MSc Thesis, University of Auckland, Auckland.

Handley, K.M., Campbell, K.A., Mountain, B.W., and Browne, P.R.L. 2005. Abiotic-biotic controls on the origin and development of spicular sinter: *in situ* growth experiments, Champagne Pool, Waiotapu, New Zealand. *Geobiology*, 3:93-114.

Healy, J. 1965. Quaternary pumice deposits, p. 61-72. In Thompson, B.N., Kermode, L.D., and Ewart, A. (eds.), *New Zealand Volcanology, Central Volcanic Zone*. Department of Scientific and Industrial Research, Series 50, Wellington.

Henley, R.W. 1996. Chemical and physical context for life in terrestrial hydrothermal systems: chemical reactors for the early development of life and hydrothermal ecosystems, p. 61-82. In Bock, G.R. and Goode, J.A. (eds.), *Evolution of Hydrothermal Ecosystems on Earth (and Mars?), Ciba Foundation Symposium 202*. John Wiley and Sons, Chichester.

Herdianita, N.R., Rodgers, K.A., and Browne, P.R.L. 2000a. Routine instrumental procedures to characterise the mineralogy of modern and ancient sinter. *Geothermics*, 29:65-81.

Herdianita, N.R., Browne, P.R.L., Rodgers, K.A., and Campbell, K.A. 2000b. Mineralogical and textural changes accompanying ageing of siliceous sinter. *Mineralium Deposita*, 35:48-62.

Hinman, N.W. and Lindstrom, R.F. 1996. Seasonal changes in silica deposition in hot spring systems. *Chemical Geology*, 132:237-246.

Hostetter, H.P. and Hoshaw, R.W. 1970. Environmental factors affecting resistance to desiccation in the diatom *Stauroneis anceps. American Journal of Botany*, 57:512-518.

Hugenholtz, P., Pitulle, C., Herschenberger, K.L., and Pace, N.R. 1998. Novel division level bacterial diversity in a Yellowstone hot spring. *Journal of Bacteriology*, 180:366-376.

Iler, R.K. 1979. *The chemistry of silica: solubility, polymerization, colloid and surface properties and biochemistry*. Wiley, New York.

Inagaki, F., Motomura, Y., Doi, K., Taguchi, S., Izawa, E., Lowe, D.R., and Ogata, S. 2001. Silicified microbial community from at Steep Cone Hot Spring, Yellowstone National Park. *Microbes and Environment*, 16:125-130.

Jones, B. and Renaut, R.W. 1997. Formation of silica oncoids around geysers and hot prings at El Tatio, northern Chile. *Sedimentology*, 44:287-304.

Jones, B. and Renaut, R.W. 2003. Petrography and genesis of spicular and columnar geyserite from the Whakarewarewa and Orakeikorako geothermal areas, North Island, New Zealand. *Canadian Journal of Earth Sciences*, 40:1585-1610.

Jones, B. and Renaut, R.W. 2004. Water content of opal-A: implications for the origin of laminae in geyserite and sinter. *Journal of Sedimentary Research*, 74:117-128.

Jones, B., Renaut, R.W., and Konhauser, K.O. 2005. Genesis of large siliceous stromatolites at Frying Pan Lake, Waimangu geothermal field, North Island, New Zealand. *Sedimentology*, 52:1229-1252.

Jones, B., Renaut, R.W. and Rosen, M.R. 1999. Role of fungi in the formation of siliceous coated grains, Waiotapu geothermal field, North Island, New Zealand. *Palaios*, 14:475-492.

Jones, B., Renaut, R.W. and Rosen, M.R. 2000. Stromatolites forming in acidic hot-spring waters, North Island, New Zealand. *Palaios*, 15:450-475.

Kerr, R.A. 2004. Rainbow of Martian minerals paints picture of degradation. *Science*, 305:770-771.

Konhauser, K.O. and Ferris, F.G. 1996. Diversity of iron and silica precipitation by microbial mats in hydrothermal waters, Iceland: implications for Precambrian iron formations. *Geology*, 24:323-326.

Konhauser, K.O., Jones, B., Phoenix, V.R., Ferris, G. and Renaut, R.W. 2004. The microbial role in hot spring silicification. *Ambio*, 33:552-558.

Konhauser, K.O., Phoenix, V.R., Bottrell, S.H., Adams, D.G., and Head, I.M. 2001. Microbial-silica interactions in Icelandic hot spring sinter: possible analogues for some Precambrian siliceous stromatolites. *Sedimentology*, 48:415-433.

Krauskopf, K.B. 1956. Dissolution and precipitation of silica at low temperatures. *Geochimica et Cosmochimica Acta*, 10:1-26.

Krumbein, W.E. 1983. Stromatolites: the challenge of a term in time and space. *Precambrian Research*, 20:493-531.

Krupp, R.E., Browne, P.R.L., Henley, R.W., and Seward, T.M. 1986. Rotokawa Geothermal Field, p. 47-55. In Henley, R.W., Hedenquist, J.W., and Roberts, P.J. (eds.), *Guide to the Active Epithermal (Geothermal) Systems and Precious Metal Deposits of New Zealand, Monograph Series on Mineral Deposits, Volume 26.* Gebrüder Borntraeger, Stuttgart.

Krupp, R.E. and Seward, T.M. 1987. The Rotokawa geothermal system, New Zealand. *Economic Geology*, 82:1109-1129.

Laclair, D.A. and Benison, K.C. 2002. Acid environments on Mars?: the physical sedimentology. *The Geological Society of America, Denver Annual Meeting*, 34:175

Lalonde, S.V., Konhauser, K.O., Reysenbach, A.-L., and Ferris, F.G. 2005. The experimental silicification of Aquificales and their role in hot spring sinter formation. *Geobiology*, 3:41-52.

Le Magrex-Debar, E., Lemoine, J., Gelle, M.P., Jaqueline, L.F., and Choisy, C. 2000. Evaluation of biohazards in dehydrated biofilms on foodstuff packaging. *International Journal of Food Microbiology*, 5:239-243.

Lowe, D.R. and Braunstein, D. 2003. Microstructure of high-temperature (>73°C) siliceous sinter deposited around hot springs and geysers, Yellowstone Park: the role of biological and abiological processes in sedimentation. *Canadian Journal of Earth Sciences*, 40:1611-1642.

Lowe, D.R., Anderson, K.S., and Braunstein, D., 2001. The zonation and structuring of siliceous sinter around hot springs, p. 143-166. In Reysenbach, A.-L., Voytek, M., and Mancinelli, R. (eds.), *Thermophiles: Biodiversity, Ecology and Evolution*. Kluwer Academic/Plenum Publishers, New York.

Luttenton, M.R. and Rada, R.G. 1986. Effects of disturbance on epiphytic community architecture. *Journal of Phycology*, 22:320-326.

Lynne, B.Y. and Campbell, K.A. 2003. Diagenetic transformations (opal-A to quartz) of low- and mid-temperature microbial textures in siliceous hot-spring deposits, Taupo Volcanic Zone, New Zealand. *Canadian Journal of Earth Sciences*, 40:1679-1696.

Lynne, B.Y. and Campbell, K.A. 2004. Morphologic and mineralogic transitions from opal-A to opal-CT in low-temperature siliceous sinter diagenesis, Taupo Volcanic Zone, New Zealand. *Journal of Sedimentary Research*, 74:561-579.

Makrides, A.C., Turner, M., and Slaughter, J. 1980. Condensation of silica from supersaturated silicic acid solutions. *Journal of Colloid and Interface Science*, 73:345-367.

Marshall, W.L. and Chen, C.-T.A. 1982. Amorphous silica solubilities – VI. Postulated sulfate-silicic acid solution complex. *Geochimica et Cosmochimica Acta*, 46:367-370.

McCollom, T.M. and Hynek, B.M. 2005. A volcanic environment for bedrock diagenesis at Meridiani Planum on Mars. *Nature*, 438:1129-1131.

McNeill, K. and Hamilton, I.R. 2003. Acid tolerance response of biofilm cells of *Streptococcus mutans*. *FEMS Microbiology Letters*, 221:25-30.

Moore, L.S. and Burne, R.V. 1994. The modern thrombolites of Lake Clifton, Western Australia, p. 3-29. In Bertrand-Sarfati, J. and Monty, C. (eds.), *Phanerozoic Stromatolites II*. Kluwer Academic Publishers, Boston.

Mountain, B.W., Benning, L.G., and Boerema, J.A. 2003. Experimental studies on New Zealand hot spring sinters: rates of growth and textural development. *Canadian Journal of Earth Sciences*, 40:1643-1667.

Pace, N.R. 1997. A molecular view of microbial diversity and the biosphere. *Science*, 276:734-740.

Pancost, R.D., Pressley, S., Coleman, J.M., Benning, L.G., and Mountain B.W. 2005. Lipid biomolecules in silica sinters: indicators of microbial biodiversity. *Environmental Microbiology*, 7:66-77.

Pancost, R.D., Pressley S., Coleman, J.M., Talbot., H.M., Kelly, S.P., Farrimond, P., Schouten, S., Benning, L., and Mountain, B.W. 2006. Composition and implications of diverse lipids in New Zealand geothermal sinters. *Geobiology*, 4:71-92.

Purevdorj, B., Costerton, J.W., and Stoodley, P. 2002. Influence of hydrodynamics and cell signaling on the structure and behavior of *Pseudomonas aeruginosa* biofilms. *Applied and Environmental Microbiology*, 68:4457-4464.

Renaut, R.W., Jones, B., and Tiercelin, J.-J. 1998. Rapid *in situ* silicification of microbes at Loburu hot springs, Lake Bogoria, Kenya Rift Valley. *Sedimentology*, 45:1083-1103.

Reyes, A.G., Trompetter, W.J., Britten, K., and Searle, J. 2002. Mineral deposits in the Rotokawa geothermal pipelines, New Zealand. *Journal of Volcanology and Geothermal Research*, 119:215-239.

Rice, C.M., Ashcroft, W.A., Batten, D.J., Boyce, A.J., Caulfield, J.B.D., Fallick, A.E., Hole, M.J., Jones, E., Pearson, M.J., Rodgers, G., Saxton, J.M., Stuart, F.M., Trewin, N.H., and Turner, G. 1995. A Devonian auriferous hot spring system, Rhynie, Scotland. *Journal of the Geological Society, London*, 152:229-250.

Rimstidt, J.D. and Cole, D.R. 1983. Geothermal mineralization I: the mechanism of formation of the Beowawe, Nevada, siliceous sinter deposit. *American Journal of Science*, 283:861-875.

Rodgers, K.A., Browne, P.R.L., Buddle, T.F., Cook, K.L., Greatrex, R.A., Hampton, W.A., Herdianita, N.R., Holland, G.R., Lynne, B.Y., Martin, R., Newton, Z., Pastars, D., Sannazzaro, K.L., and Teece, C.I.A. 2004. Silica phases in sinters and residues from geothermal fields of New Zealand. *Earth Science Reviews*, 66:1-61.

Rodgers, K.A., Cook, K.L., Browne, P.R.L., and Campbell, K.A. 2002. The mineralogy, texture and significance of silica derived from alteration by steam condensate in three New Zealand fields. *Clay Minerals*, 37:299-322.

Schinteie, R. 2005. *Siliceous sinter facies and microbial mats from acid-sulphate-chloride springs, Parariki Stream, Rotokawa Geothermal Field, Taupo Volcanic Zone, New Zealand*. Unpublished MSc Thesis, University of Auckland, Auckland.

Schultze-Lam, S., Ferris, F.G., Konhauser, K.O., and Wiese, R.G. 1995. *In situ* silicification of an Icelandic hot spring microbial mat: implications for microfossil formation. *Canadian Journal of Earth Sciences*, 32:2021-2026.

Seckbach, J. 1998. The cyanidiophyceae: hot spring acidophilic algae, p. 427-435. In Seckbach, J. (ed.), *Enigmatic microorganisms and life in extreme environments.* Kluwer Academic Publishers, Boston.

Semikhatov, M.A., Gebelein, C.D., Cloud, P., Awramik, S.M., and Benmore, W.C. 1979. Stromatolite morphogenesis: progress and problems. *Canadian Journal of Earth Sciences*, 19:992-1015.

Simmons, S. and Norris, P.R. 2002. Acidophiles of saline water at thermal vents of Volcano, Italy. *Extremophiles*, 6:201-207.

Stetter, K.O. 1996. Hyperthermophiles in the history of life, p. 1-10. In Bock, G.R. and Goode, J.A. (eds.), *Evolution of Hydrothermal Ecosystems on Earth (and Mars?), Ciba Foundation Symposium 202*. John Wiley and Sons, Chichester.

Stoddart, D.R. and Scoffin, T.P. 1979. Microatolls: review of form, origin and terminology. *Atoll Research Bulletin*, 224:1-17.

Stoodley, P., Sauer, K., Davies, D.G., and Costerton, J.W. 2002. Biofilms as complex differentiated communities. *Annual Review of Microbiology*, 55:187-209.

Sutherland, I.W. 2001. Biofilm exopolysaccharides: a strong and sticky framework. *Microbiology*, 147:3-9.

Teece, C.I.A. 2000. *Sinters deposited from acid-sulfate chloride waters at the Rotokawa geothermal field (Taupo Volcanic Zone, New Zealand)*. Unpublished MSc Thesis, University of Auckland, Auckland.

Teitzel, G.M. and Parsek, M.R. 2003. Heavy metal resistance of biofilm and planktonic *Pseudomonas aeruginosa*. Applied and Environmental Microbiology, 61:2313-2320.

Toporski, J., Steele, A., Westall, F., Thomas-Keprta, K.L., and McKay, D.S. 2002. The simulated silicification of bacteria – new clues to the modes and timing of bacterial preservation and implications for the search for extraterrestrial microfossils. *Astrobiology*, 2:1-26.

Trewin, N.H., Fayers, S.R., and Kelman, R. 2003. Subaqueous silicification of the contents of small ponds in an Early Devonian hot-spring complex, Rhynie, Scotland. *Canadian Journal of Earth Sciences*, 40:1697-1712.

Vucetich, C.G. and Pullar, W.A. 1973. Holocene tephra formations erupted in the Taupo Area, and interbedded tephras from other volcanic sources. *New Zealand Journal of Geology and Geophysics*, 16:745-780.

Walker, J.J., Spear, J.R., and Pace, N.R. 2005. Geobiology of a microbial endolithic community in the Yellowstone geothermal environment. *Nature*, 434:1011-1014.

Walter, M.R. 1976. Geyserites of Yellowstone National Park: an example of abiogenic "stromatolites," p. 87-112. In Walter, M.R. (ed.), *Stromatolites*. Elsevier, Amsterdam.

Walter, M.R., Des Marais, D., Farmer, J.D., and Hinman, N.W. 1996. Lithofacies and biofacies of Mid-Paleozoic thermal spring deposits in the Drummond Basin, Queensland, Australia. *Palaios*, 11:497-518.

Walter, M.R. and Des Marais, D.J. 1993. Preservation of biological information in thermal spring deposits: developing a strategy for the search for fossil life on Mars. *Icarus*, 101:129-143.

Walter, M.R., Bauld, J., and Brock, T.D. 1972. Siliceous algal and bacterial stromatolites in hot spring and geyser effluents of Yellowstone National Park. *Science*, 178:402-405.

Weed, W.H. 1889. Formation of travertine and siliceous sinter by the vegetation of hot springs. *United States Geological Survey, 9th Annual Report*, 613-676.

Weres, O., Yee, A., and Tsao, L. 1981. Kinetics of silica polymerization. *Journal of Colloid and Interface Science*, 84:379-402.

Westall, F., Boni, L., and Guerzoni, E. 1995. The experimental silicification of microorganisms. *Palaeontology*, 38:495-528.

White, D.E., Brannock, W.W., and Murata, K.J. 1956. Silica in hot-spring waters. *Geochimica et Cosmochimica Acta*, 10:27-59.

Wilson, C.J.N., Houghton, B.F., McWilliams, M.O., Lanphere, M.A., Weaver, S.D., and Briggs, R.M. 1995. Volcanic and structural evolution of Taupo Volcanic Zone: a review. *Journal of Volcanology and Geothermal Research*, 68:1-28.

Yee, N., Phoenix, V.R., Konhauser, K.O., Benning, L.G., and Ferris, F.G. 2003. The effects of cyanobacteria on silica precipitation at neutral pH: implications for bacterial silicification in geothermal hot springs. *Chemical Geology*, 199:83-90.